electronics

MDPI

Article

Efficiency Measurements of Energy Harvesting from Electromagnetic Environment for Selected General Purpose Telecommunication Systems

Kazimierz Kamuda, Dariusz Klepacki *, Wiesław Sabat, Kazimierz Kuryło, Mariusz Skoczylas and Piotr Jankowski-Mihułowicz *

Department of Electronic and Telecommunications Systems, Rzeszow University of Technology, W. Pola 2, 35-959 Rzeszow, Poland; kazik@prz.edu.pl (K.K.); wsabat@prz.edu.pl (W.S.); kkurylo@prz.edu.pl (K.K.); msko@prz.edu.pl (M.S.)

* Correspondence: dklepa@prz.edu.pl (D.K.); pjanko@prz.edu.pl (P.J.-M.)

Abstract: The results of measurements of the efficiency of energy harvesting from commonly available general-purpose telecommunications systems, divided into typical bands available under European conditions, have been presented in this paper. Specially designed harvesters were used, dedicated to powering autonomous semi-passive Radio Frequency Identification (RFID) tags. For the assumed resistive loads, the achievable output voltage values of the harvesters were measured across a wide spectrum of electromagnetic field strengths, simulating real conditions. The performance and dynamics of the energy storage process with fixed parameters were studied at an intermediate stage, before the energy conditioning process. The harvesters were treated as typical energy sources with unknown but variable parameters, so their dynamic parameters and instantaneous energy supply were also analyzed. These activities will enable the final development of a power supply system with parameters acceptable for the planned applications and whose efficiency will be maximized under the given conditions. For this purpose, the energy harvesting systems were designed, a suitable laboratory stand was built, and the elaborated circuits were measured to determine the expected parameters of energy harvesting.

Keywords: energy harvesting; RFID systems; telecommunication systems

Citation: Kamuda, K.; Klepacki, D.; Sabat, W.; Kuryło, K.; Skoczylas, M.; Jankowski-Mihułowicz, P. Efficiency Measurements of Energy Harvesting from Electromagnetic Environment for Selected General Purpose Telecommunication Systems. *Electronics* **2024**, *13*, 3111. https://doi.org/10.3390/electronics13163111

Academic Editors: Joao L. Afonso, Vítor Monteiro, José A. Afonso and João Paulo Pereira do Carmo

Received: 6 June 2024
Revised: 17 July 2024
Accepted: 2 August 2024
Published: 6 August 2024

1. Introduction

Currently, there is a global increase in the number of various radio and television communication systems, which is driven by technological development. The operation of these systems is inseparable from the conscious emission of electromagnetic energy carrying useful information (radio, television, data communication transmitters, etc.). Today, with the significant burden on the natural electromagnetic environment, the issue of electromagnetic smog has become a serious concern, particularly in large cities [1]. This degree of overloading the environment with electromagnetic energy both from intentional and nonintentional systems enabled the realization of the theory formulated at the end of the last century regarding supplying sensors or electronic biomedical components [2–7].

The Internet of Things (IoT) has also become a rapidly growing field, where energy harvesting and storage systems have also found their possible applications [8–10].

According to the concept of harvesting, energy can be extracted, stored, and reused to power a selected class of electronic circuits, especially those which require minimal energy for proper operation. This type of energy can be considered in the frequency domain. In the dedicated frequency bands used by Information and Communication Technologies (ICT) systems, the energy concentration of about -25 dBm/m^2 allows for its harvesting. The energy for harvesting can be obtained mainly from mobile phone (GSM) systems, wireless network systems (WiFi), terrestrial TV systems, and from radio broadcast systems [11,12].

Modern mobile phone systems represent a potential source of energy harvesting. The energy harvesting possibilities are strongly dependent on the power of their transmitters. This parameter along with adequate frequency are defined in the standards of particular GSM systems. The extent of electromagnetic fields with threshold values around mobile base station antennas is determined by the power fed into these antennas and their radiation properties. In the vicinity around standard mobile telephony base stations, electromagnetic fields with threshold values are present within a few tens of meters from the antennas and at their installation height. This distance of several tens of meters is relevant only along the axes of the main radiation beams of the antennas [13–16].

In the electromagnetic environment, terrestrial television systems (currently primarily digital) play an important role. To achieve the maximum possible range, antenna masts are usually erected at significant height relative to ground level (up to 50 m), often using natural hills. The strengths of the permissible electromagnetic field in the vicinity of radiocommunication equipment depend on the frequency of operation of equipment, the radiation characteristics of antennas, the height of their suspension, and, most importantly on the power [17].

WiFi data networks operating on the IEEE 802.11 standard [18] could serve as another potential source for energy harvesting. This standard includes several variations (the most popular being 802.11a, b, g, n, and ac). The 802.11.ac version has data transmission rates as low as 1 Gbps. This standard uses publicly available frequencies, ranging from 2.4 GHz (in 802.11b and 802.11g) to 5.2 GHz (in 802.11a), which results in specific restrictions on the permissible power values of the transmitted signals. Wireless local area networks are most often designed within buildings; wave propagation in such an environment is quite specific due to the numerous barriers present along the propagation path [19].

The multitude of potential sources of recoverable energy from the electromagnetic environment has attracted significant interest from commercial companies specializing in harvester systems and energy storage methods. However, realistically, few companies offer ready-made, commercial solutions. The biggest player in the RF harvester market is PowerCast, which supplies ready-to-use modules. Another company is e-Pass, which offers the AEM30940 module for harvesting energy from the electromagnetic environment. Other companies offering various solutions for IoT and using harvested energy from the environment include Energous, GuRu, and Ossia. A comprehensive study of commercially available harvester systems together with the developed simulation models can be found in [20].

As part of this study, the harvester circuit of the P21XXCSR evaluation kit developed by PowerCast Corporation was tested. The circuit was designed by the authors as the main component responsible for extracting energy from common telecommunication systems for a semi-passive RFID tag [21]. The capabilities of the circuit were investigated in terms of achievable output voltages for different field strength levels and sample antennas with different characteristics. Load resistances were determined based on source–receiver matching and maximizing the power received from the harvester system. The influence of signal frequency on energy recovery was also examined within the specified parameters. In the next stage, tests were conducted to determine the time parameters of the energy storage process, such as capacitances of storage capacitors and the dynamics of this process (for example, capacitances of 10 μF, 100 μF, and 1000 μF). The resulting data, obtained under conditions corresponding to the real environment, allowed for the selection of parameters for the energy conditioning and storage systems to maximize the amount of energy obtained in the energy recovery process.

The paper is structured into six sections. Section 2 details the test circuits used for investigations with focus on operational output parameters. Section 3 outlines the methodology of measurements. Sections 4 and 5 analyze and discuss the obtained results. Section 6 concludes with an outline of future work.

2. Test Circuit

The P21XXCSR circuit was selected as the harvester circuit for the energy recovery and storage system of the designed semi-passive identifier. This specially designed chip operates within frequencies ranging from 824 to 2495 MHz across several sub-bands (Table 1), allowing us to verify the harvester system parameters under real conditions across a wide spectrum of potential energy recovery sources (GSM, DCS, UMTS, Wi-Fi bands) available in European conditions. An overview of the system concept is presented in Figure 1.

Table 1. Operating frequencies of the Powercast Corporation P21XXCSR harvester system [22].

Component	Band	Band (MHz)	Center Frequency (MHz)
J1	GSM-850 uplink	824–849	836.5
J2	Europe RFID and GSM-850 downlink	865–894	879.5
J3	GSM-900 and EGSM-900	925–960	947.5
J4	GSM-1800 uplink	1710–1785	1747.5
J5	GSM-1800/LTE downlink	1805–1825	1815
J6	WiFi 2.4 GHz (ETSI)	2400–2495	2442

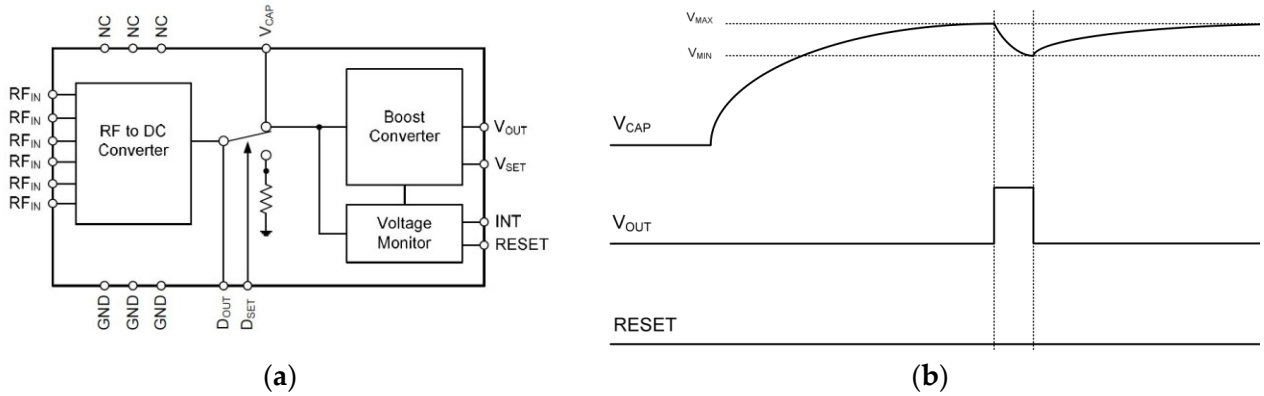

Figure 1. Block diagram of the P21XXCSR system from Powercast Corp. (**a**) and an illustration of the operating principle of the energy storage charging inverter (**b**) [22].

The HF voltage from the antenna is directed to rectifiers built on Shottky diodes (RF to DC CONVERTER). The rectified voltage recharges a capacitor placed at the rectifier output connected to the V_{CAP} output. The voltage in the capacitor is controlled by the voltage detector circuit (VOLTAGE MONITOR). When the voltage exceeds a preset threshold, a voltage converter (BOOST CONVERTER) is activated to ensure optimum performance of the main energy storage, typically utilizing supercapacitors. The converter draws energy from the capacitor connected to the V_{CAP} output, regulates the maximum output voltage of the circuit V_{MAX}, and operates until the voltage drops below the minimum voltage V_{MIN} in the capacitor. The aforementioned energy storage can be optionally connected to the output of the inverter, storing energy to supply external circuits. During testing, the output voltages (V_{MAX} and V_{MAX}) of the converter can be adjusted. Under typical operation conditions, the DC power output is monitored by one of three voltage detectors, selectable at thresholds of 1.2 V, 0.9 V, or 0.7 V via JP3, JP4, or JP5, respectively. The storage capacitor, chosen via JP1, charges up to the selected threshold voltage. When VCAP reaches its maximum value (VMAX), INT is set high, the boost converter turns on, and VOUT is set to the output voltage selected via S1 (4.2 V, 4.1 V, or default). The storage capacitor then

discharges until VCAP reaches its minimum value (VMIN) and then sets INT low, shutting off the boost converter until VCAP charges back up to its maximum value [22].

For testing purposes, it is also possible to change the capacitance of the capacitor at the output V_{CAP} and to disconnect the LEDs (D1–D6) in the individual harvester modules (Figure 2). A general view of the development board is presented in Figure 3.

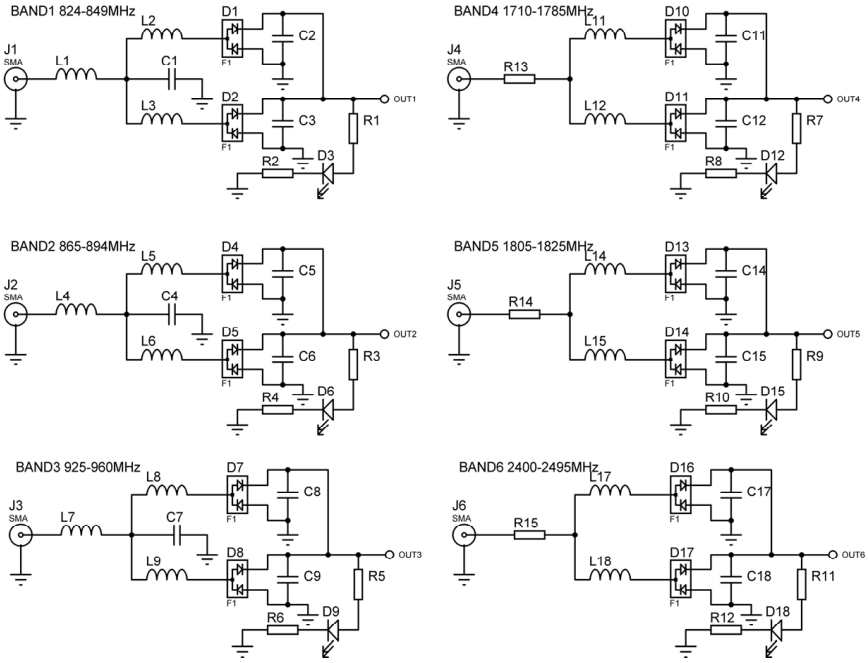

Figure 2. Schematic diagram of the P21XXCSR test module from Powercast Corp. with the capacitor C, which is connected as the load on the harvester system when its dynamic parameters are measured by authors (according to Figure 3, this can be C1, C2, or the external component under test C3 selected by JP1, respectively).

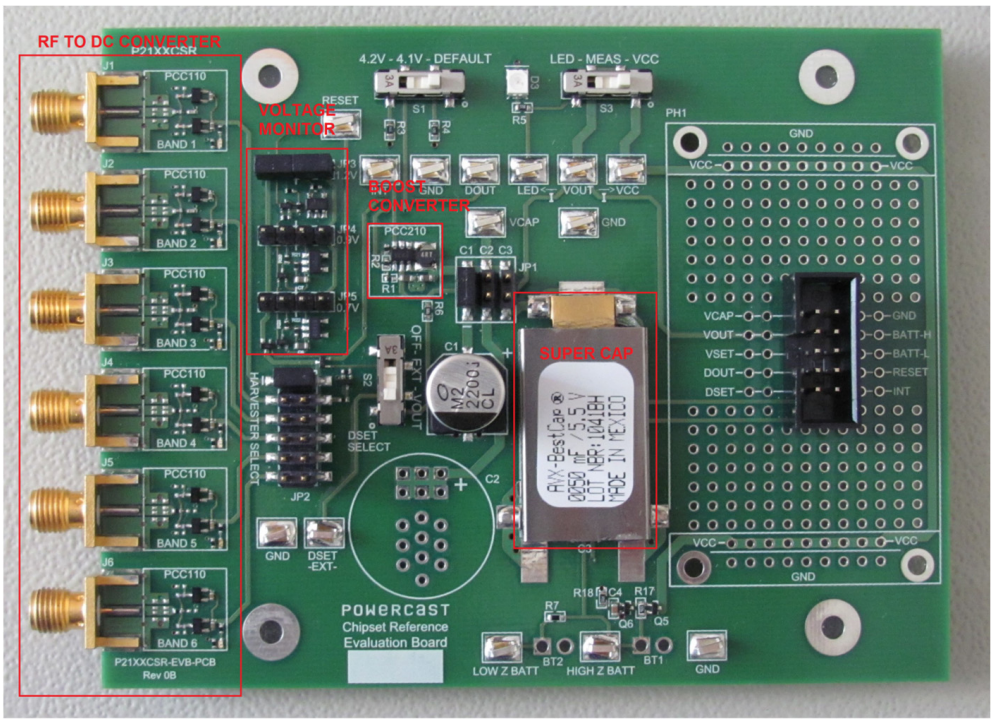

Figure 3. View of the P21XXCSR test module from Powercast Corp.

Details of the Powercast Corp. P21XXCSR evaluation board can be found in the design assumptions and technical specifications of the test module built for this study [22].

3. Methodology and Test Setup

Taking advantage of the field homogeneity in the measurement area of the anechoic chamber, it was assumed that the measurement system could be significantly simplified and work could be accelerated by leveraging the known characteristics and symmetry of the antenna. As presented in Figure 4b, both the measurement probe and the device under test (harvester) were symmetrically positioned along the main axis of the antenna radiation. The distance from the axis was determined experimentally to ensure that the field strength measured by the probe remained unaffected by the presence or absence of the device under test. The symmetry of the antenna's characteristics then ensured that the signal level measured by the probe closely matches the signal level affecting the harvester, thereby minimizing mutual interference [21].

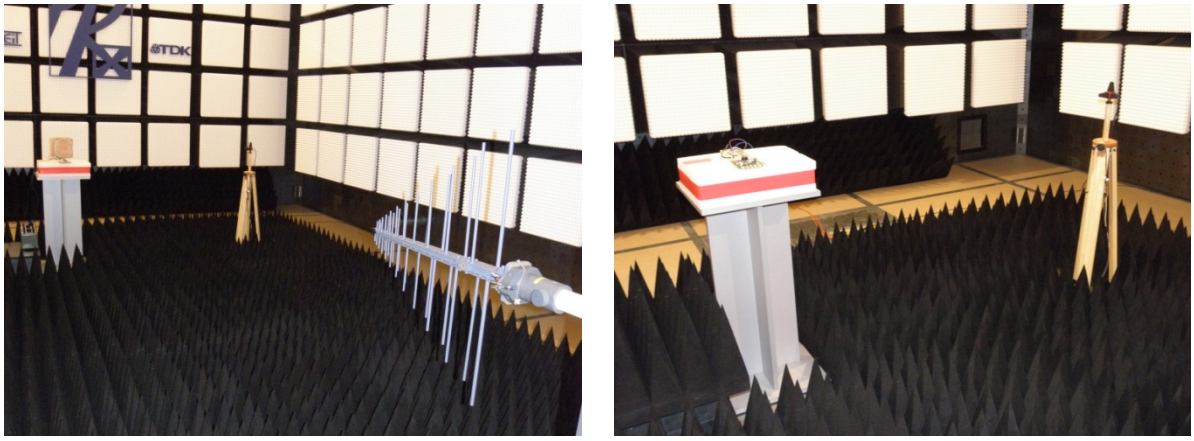

(**a**) (**b**)

Figure 4. Measurement stand for the analysis of electric field strength distribution (power density) in an anechoic chamber: (**a**) stand with HL223 antenna as the source of the electromagnetic field; (**b**) adopted concept for the measurement of field distribution—principle of symmetry of antenna radiation characteristics.

In the initial phase of the research, the output voltage of the P21XXCSR harvester system was measured as a function of the electric field strength at the antenna location of the receiver system. The measurements were conducted without overloading the energy recovery system output and with selected loads that provided useful output currents without overloading the harvester system and with an appropriate value of the output voltage. At that stage, the primary focus was to maximize the output voltage. The conducted measurements allowed for correlating the output voltage with the current flowing in the harvester's output circuit identifying an optimal load for maximizing the efficiency of the energy harvesting process. The data set were crucial for accurately determining the system's energy capabilities and establishing comprehensive and realistic scenarios of the semi-passive identifier model system. Additionally, the impact of the design and characteristics of the antenna itself, suitable for the band, was also considered.

The experiments were conducted in the TDK anechoic chamber, located within the Electromagnetic Compatibility Laboratory at the Department of Electronic and Telecommunications Systems of Rzeszów University of Technology (Poland). The choice of this test environment was driven by its suitability for testing energy acquisition model systems operating within frequency ranges commonly used by telecommunications systems, where field strengths can reach up to 5 V/m. Operating outside such controlled conditions of an anechoic chamber to generate electromagnetic fields within these frequency ranges and required strengths would violate regulatory standards. A range of equipment, including a

set of apparatus for the generation of electromagnetic fields for susceptibility tests, probes for measuring strength of these fields, and equipment for remote measurement of relevant test parameters were also used for this research. The view of the complete test setup in the anechoic chamber is presented in Figure 4. The chamber floor was lined with a set of absorbers to minimize the radiation reflected from this area and enhance the field uniformity around the tested systems, thereby mitigating the effects of multipath signal propagation from the antenna.

The primary equipment utilized in the tests was the Rohde & Schwarz EMS_1GHz system (Munich, Germany). The majority of the equipment is housed in a measurement rack, which is permanently stationed in the amplifier room adjacent to the anechoic chamber. This system comprises an SMB 100A generator, a BBA 100 power amplifier, an NRP2 power meter equipped with NRP-Z11 measuring probes from Rohde & Schwarz (refer to Figure 5), and an HL223 antenna positioned within the chamber (refer to Figure 4a).

Figure 5. View of the systems (EMS_1GHz and EMS_6GHz) by Rohde & Schwarz for the generation of electromagnetic fields at the required intensities and frequencies during operation.

To measure the strength of the generated electromagnetic fields, the ETS-Lindgren HI6005 probe was used, focusing on measuring the electric field. While the isotropic probe method employed for field measurements (utilizing the Rohde & Schwarz TS-EMF System for radiated electromagnetic field measurement, accessible at the EMC Laboratory of PRz) is recognized for its precision in determining electric field levels in the analyzed space, it is characterized by extended measurement durations. Therefore, the decision was made to utilize the HI6005 probe with slightly reduced sensitivity but with the capability of simultaneous and significantly faster measurement of all electromagnetic field components. This probe is capable of measuring electric field strength within the frequency range of 100 kHz to 6 GHz, with dynamic range spanning from 0.5 V/m to 800 V/m.

This probe offers rapid measurement capabilities (acquisition rate: one measurement of all components per second) and simultaneous analysis of all three electromagnetic field components. Its optical data exchange interface and energy system powered by laser light flux help minimize the probe's influence on measurement results.

Several antennas have been employed in the tests to analyze the impact of various characteristics of this crucial element in the energy harvesting system circuit. Powercast kits typically include two standard antenna versions, with the flexibility to attach other similarly designed devices, custom-made to meet specific specifications, using an SMA connector. Details regarding the parameters and antennas pattern utilized in the tests are provided in Table 2.

Table 2. The main parameters of the antennas tested from the Powercast Corp. P1110 harvester evaluation system.

A1	**A2**
915 MHz dipole antenna	Layer antenna 915 MHz
Omnidirectional characteristic: 360°	Directional characteristics: 122°—azimuth 68°—elevation
Vertical Polarization V	Vertical Polarization V
Energy gain: 1.25 (1.0 dBi)	Energy gain: 4.1 (6.1 dBi)
Standard evaluation kit antenna	Standard evaluation kit antenna
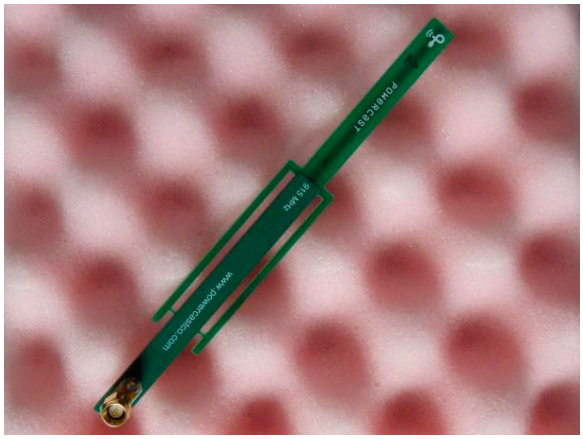	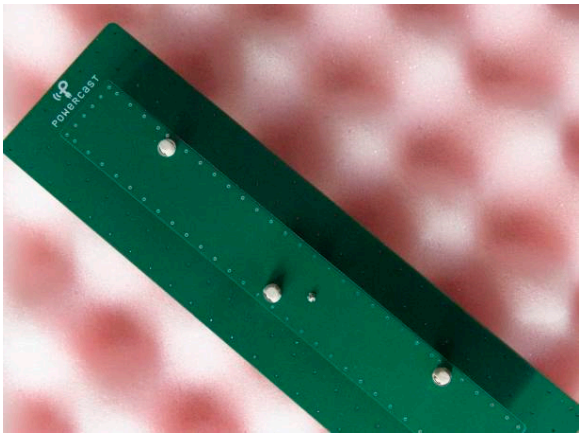
A3	**A4**
2.4 GHz circular antenna	Circular antenna with 2.4 GHz reflector
Characteristics: Ellipsoidal	Characteristics: Directional
Vertical Polarization V	Vertical Polarization V
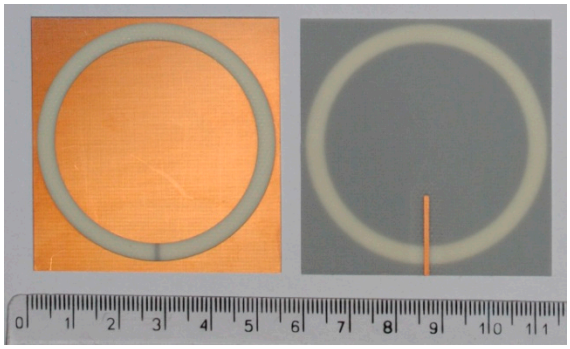	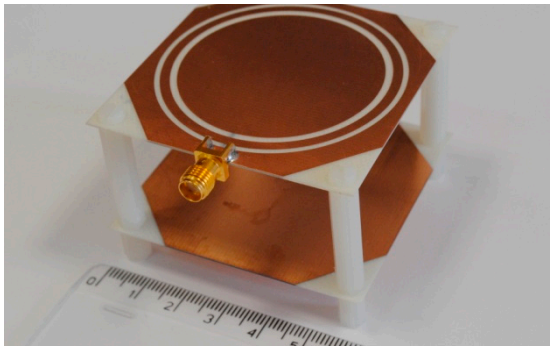

Table 2. *Cont.*

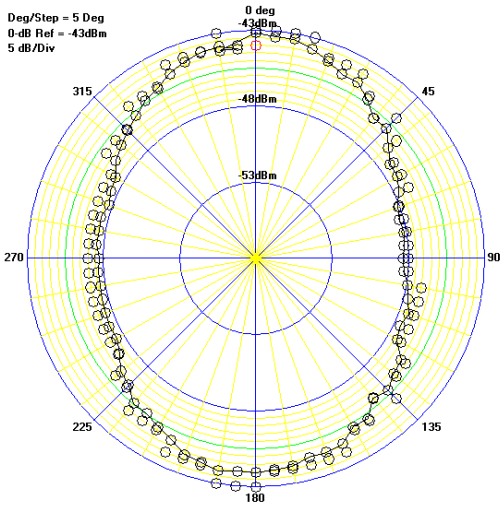	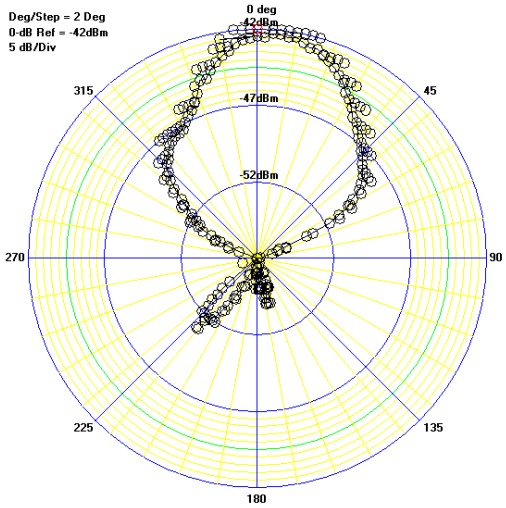
A5	**A6**
Broadband antenna PE51054 Pasternak	Circular antenna with 865 MHz reflector
Characteristics: Directional	Characteristics: Directional
Vertical Polarization V	Vertical Polarization V
Frequency range: 806–960 MHz and 1710–2500 MHz Energy gain: 7 dBi Radiation angle V: 47° Radiation angle H: 88° VSWR: <1.5:1 Sizes (W × H × D): 210 × 180 × 44 mm Weight: 470 g	
	

The evaluation board enables flexible configuration of the harvester under test, facilitating convenient testing of the harvester system in all operating modes provided by the supplier. Eventually, the harvester system will be integrated into the structure of the designed system's energy acquisition and storage system. However, during the testing phase, the adopted solution offers enhanced flexibility and allows for rapid modifications to the measurement system. Externally, the necessary components such as capacitors, load resistors, voltage and current measurement points, etc., were connected to the system under

test on a suitable prototype board. This setup is clearly visible in the final measurement system (refer to Figure 6).

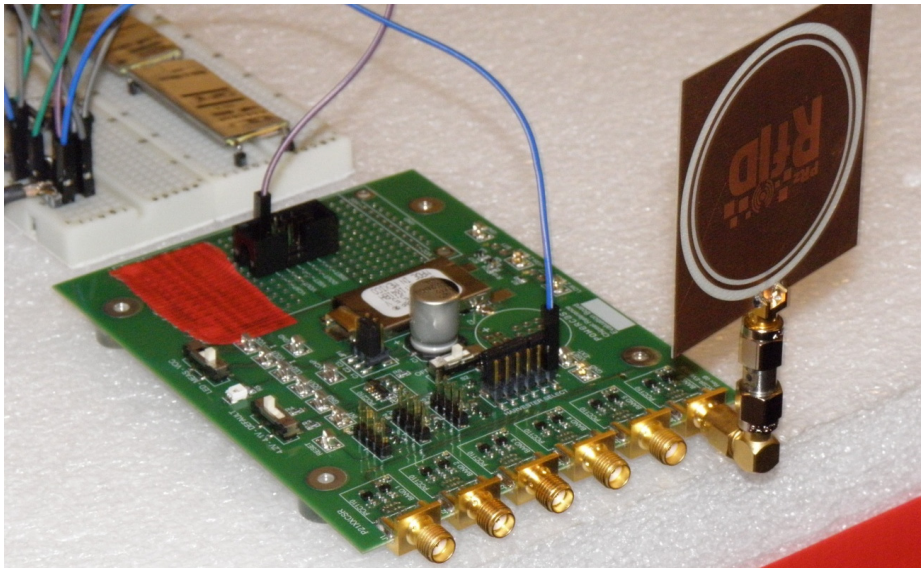

Figure 6. View of Powercast Corp.'s P21XXCSR evaluation system, prepared for testing, with the A3 type antenna installed. A test board with a set of capacitors to store recovered energy is visible in the background.

Voltage and current measurements at the test points were conducted using NI 9222 four-channel remote analog measurement data acquisition modules from National Instruments, which feature a sampling frequency of 500 ks/s and a resolution of 16 bits. The modules were housed in a shielded box within the chamber, and control and data retrieval were executed via an optical USB connection to minimize any potential adverse effects on measurement accuracy. Data were conveniently recorded using NI's SignalExpress application, facilitating processing and analysis of the measurement results.

4. Measurement Results

Based on of these measurements, several important assumptions were formulated to guide further work developing a detailed mode of operation for energy recovery systems as well as energy conditioning and storage. All described tests were conducted with consideration of the anticipated field strengths in future application areas, occasionally adjusted to gather additional data on the harvester system itself. This included varying ranges of electric field strengths (or energy densities, closely related parameters of the electromagnetic environment for steady-state conditions in the far field) adopted in individual measurements. The experimental data, referenced in [20] and obtained using the FSL analyzer and RFEX software (ver. 3.2.0) from Rohde & Schwarz, provide information on both the maximum measured electric field strength (power density) and the average value of this parameter over the analyzed time period.

During the measurements, the required field strengths for the tested band were set using the EMS_1GHz and EMS_6GHz kit software. Continuous feedback obtained from the HI6005 probe coupled with control over the output power level feeding the HL223 antenna system and checking the current standing wave ratio VSWR enabled automation of the entire process and enhanced precision of the obtained results [23]. The achieved field strengths were adequate for the system under test, while ensuring consistent and reproducible measurement conditions. The SAC chamber was previously also attenuated with absorbers with suitable characteristics.

The results of the measurements for the individual bands (at different loads and selected field strengths) are presented in Figures 7–24.

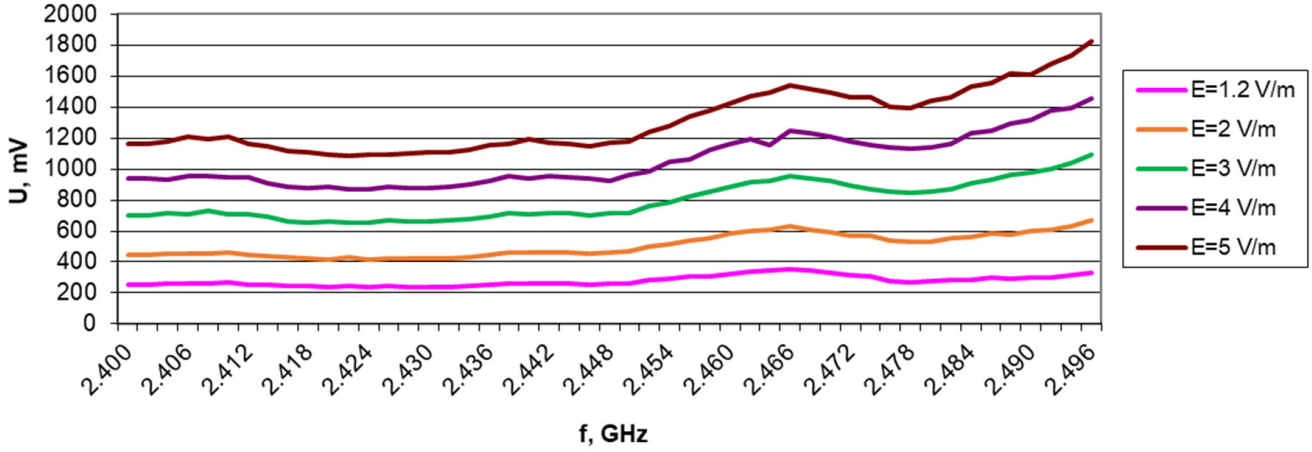

Figure 7. Results of unloaded harvester output voltage measurements for 2.4 GHz (WiFi) as a function of field strength changes for antenna A3.

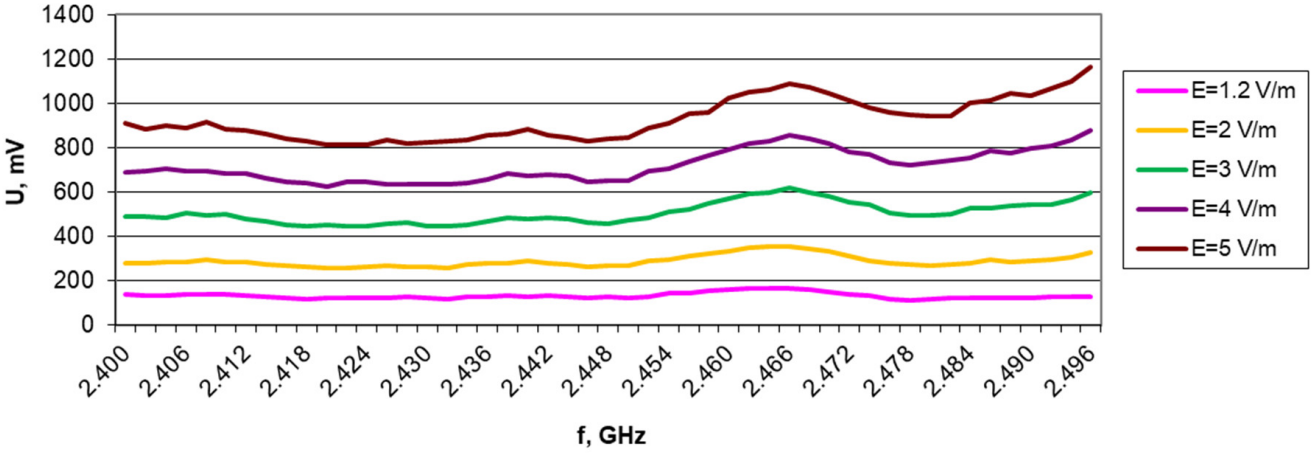

Figure 8. Results of harvester output voltage measurements with a 15 kΩ load for the 2.4 GHz band (WiFi) as a function of changes in field strength for antenna A3.

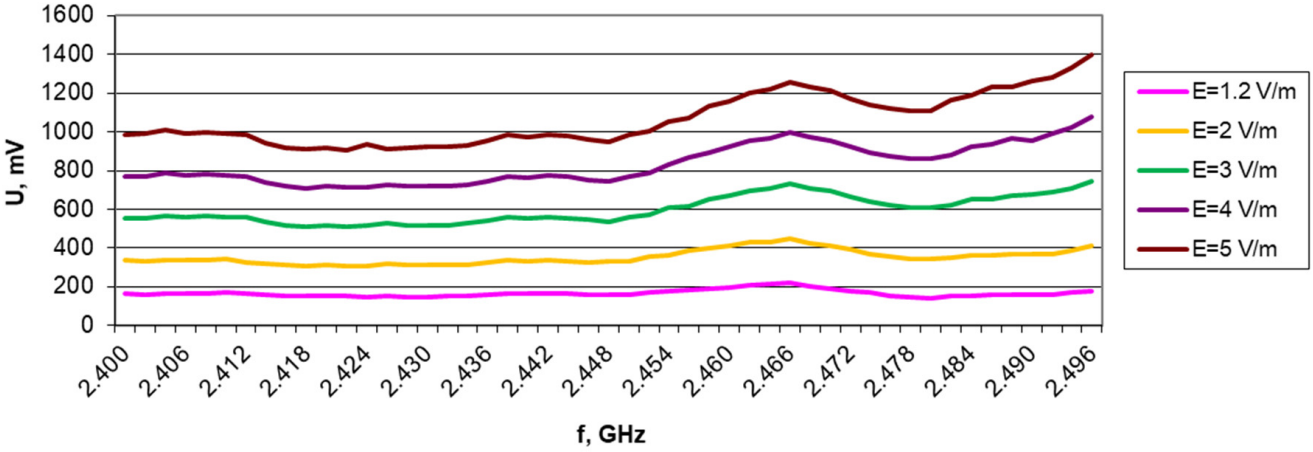

Figure 9. Results of harvester output voltage measurements with a 30 kΩ load for the 2.4 GHz band (WiFi) as a function of changes in field strength for antenna A3.

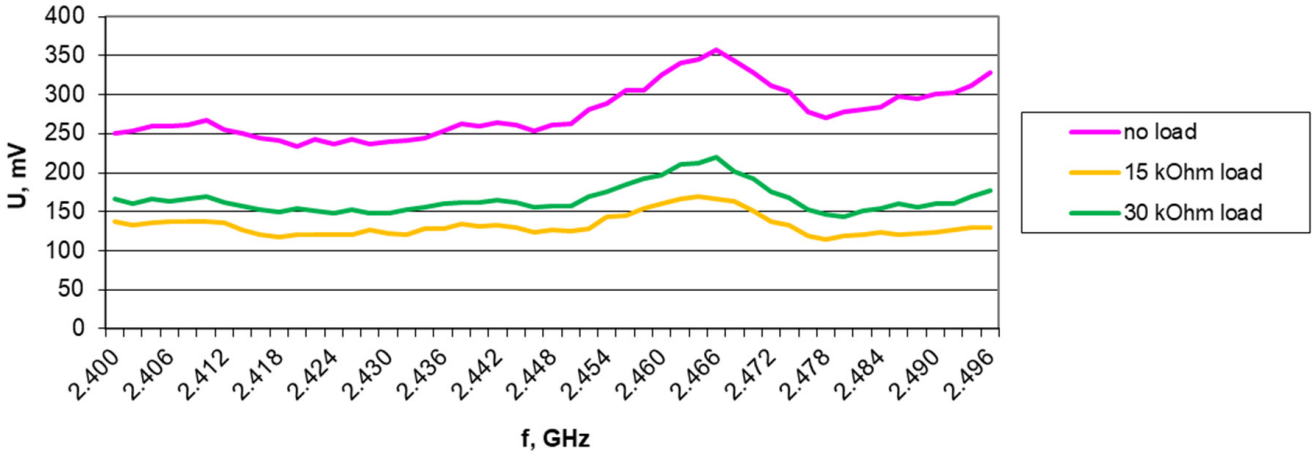

Figure 10. Results of harvester output voltage measurements without load, with 15 kΩ load, and with 30 kΩ load for the 2.4 GHz band (WiFi) in 1.2 V/m electromagnetic field of 1.2 V/m for antenna A3.

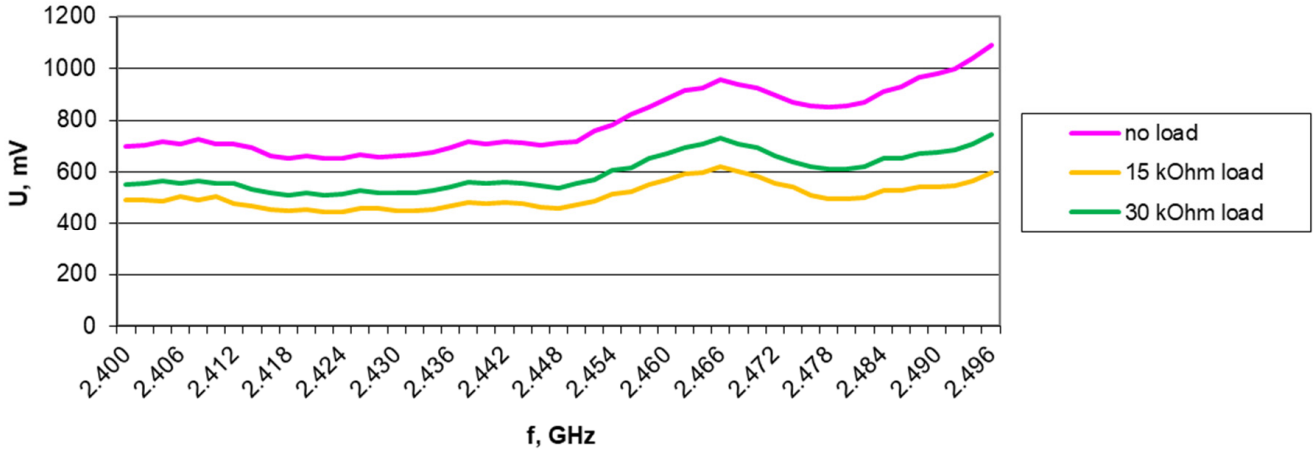

Figure 11. Results of harvester output voltage measurements without load, with 15 kΩ load, and with 30 kΩ load for the 2.4 GHz band (WiFi) in an electromagnetic field of 3 V/m for antenna A3.

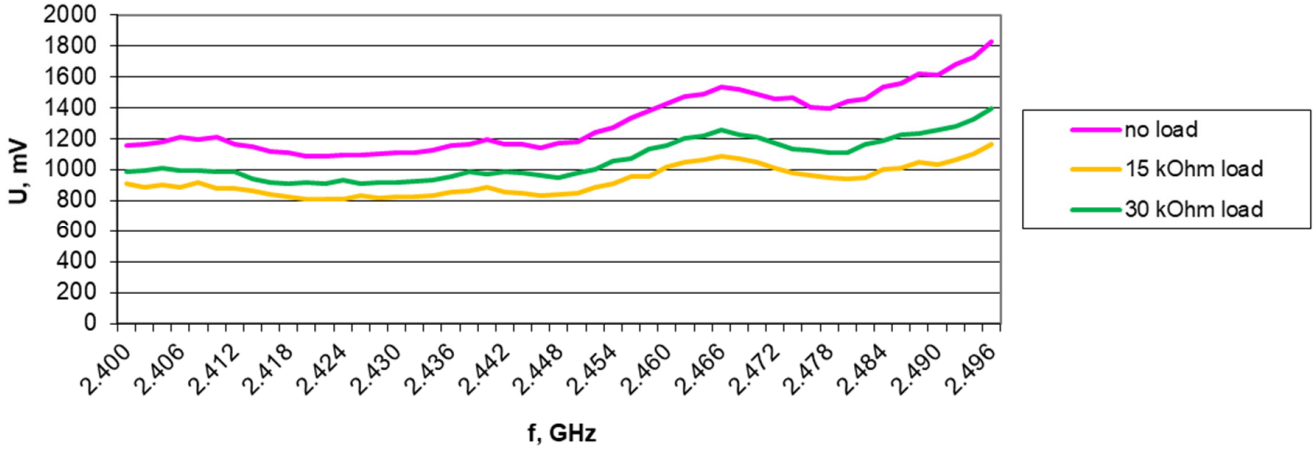

Figure 12. Results of harvester output voltage measurements without load, with 15 kΩ load, and with 30 kΩ load for the 2.4 GHz band (WiFi) in a 5 V/m electromagnetic field for antenna A3.

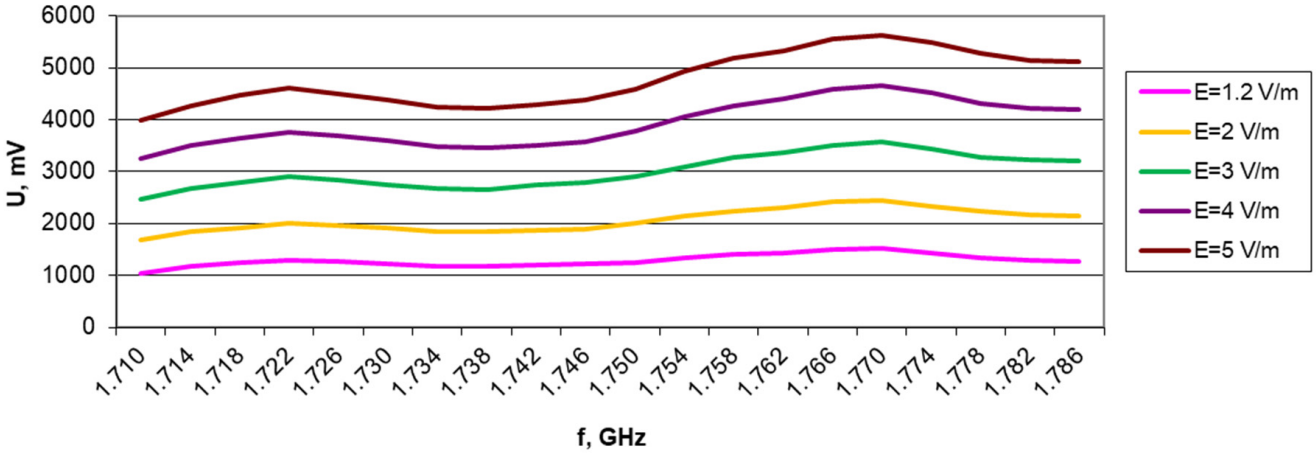

Figure 13. Results of unloaded harvester output voltage measurements for the GSM1800 band (uplink) as a function of changes in field strength for antenna A5.

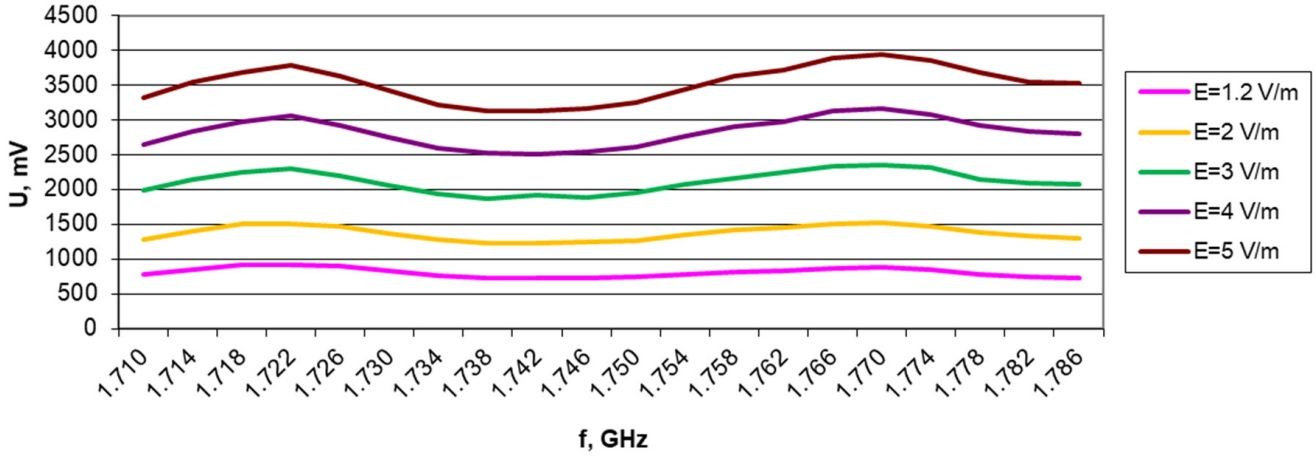

Figure 14. Results of harvester output voltage measurements with 15 kΩ load for the GSM1800 band (uplink) as a function of changes in field strength for antenna A5.

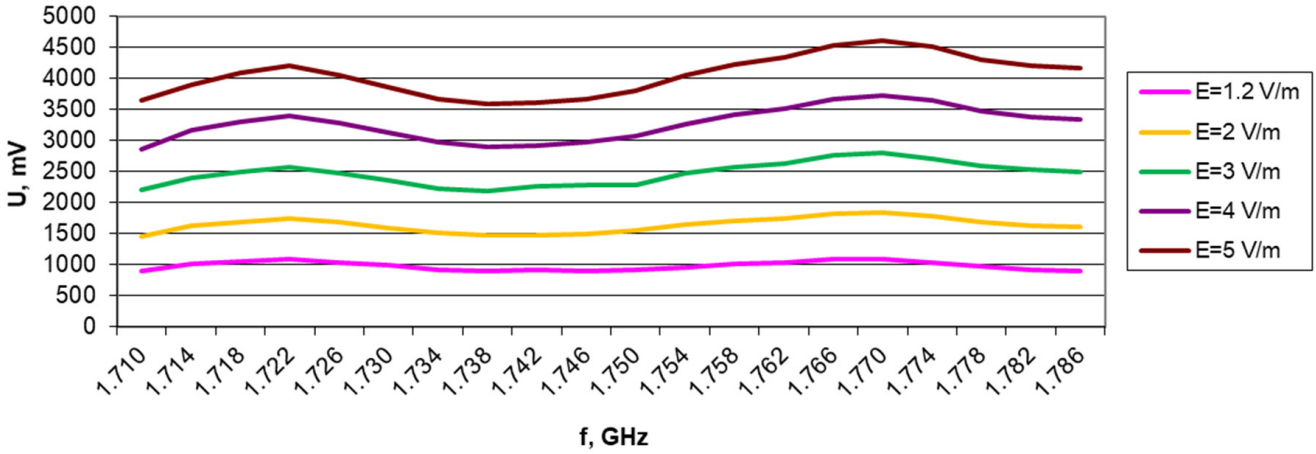

Figure 15. Results of harvester output voltage measurements with 30 kΩ load for the GSM1800 band (uplink) as a function of changes in field strength for antenna A5.

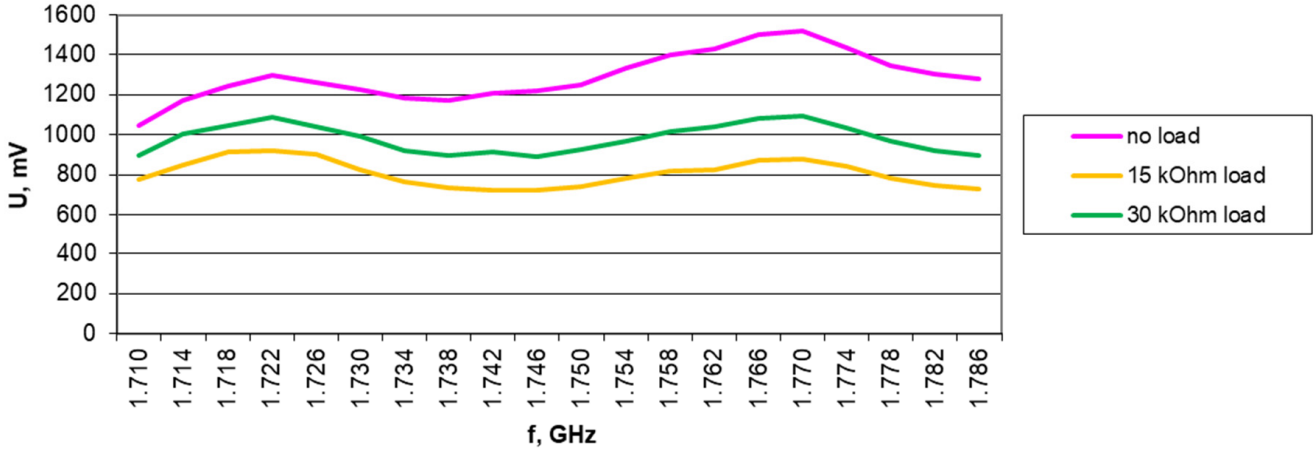

Figure 16. Results of harvester output voltage measurements without load, with 15 kΩ load, and with 30 kΩ load for the GSM1800 band (uplink) in a 1.2 V/m electromagnetic field for antenna A5.

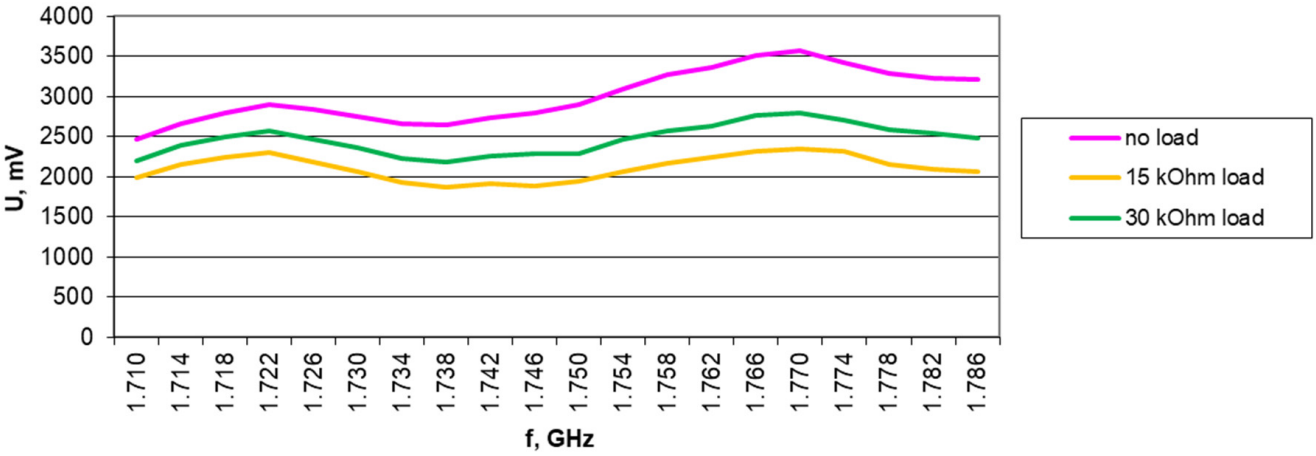

Figure 17. Harvester output voltage measurement results without load, with 15 kΩ load, and with 30 kΩ load for GSM1800 band (uplink) in an electromagnetic field of 3 V/m for antenna A5.

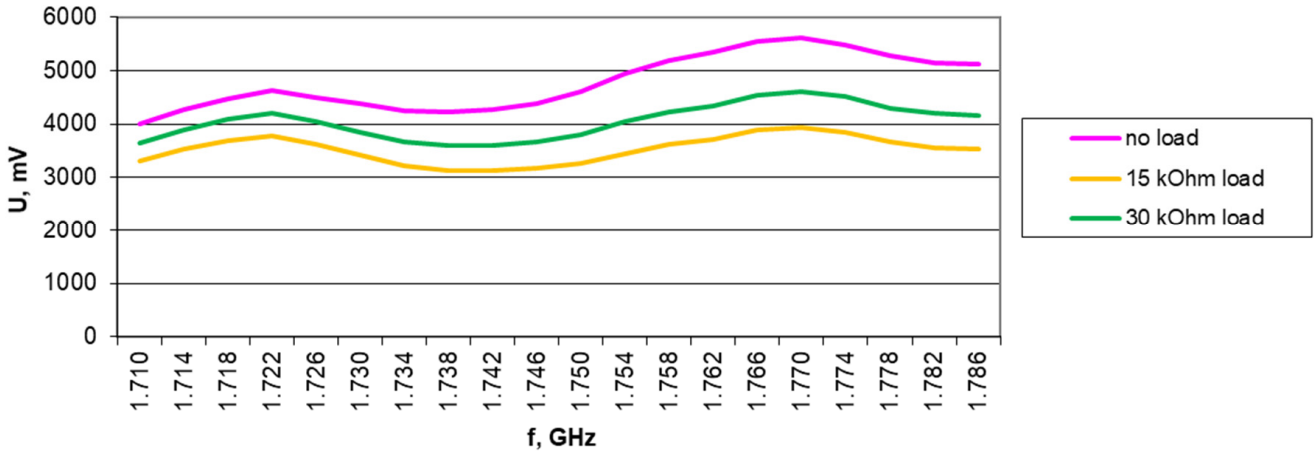

Figure 18. Harvester output voltage measurement results without load, with 15 kΩ load, and with 30 kΩ load for the GSM1800 band (uplink) in a 5 V/m electromagnetic field for antenna A5.

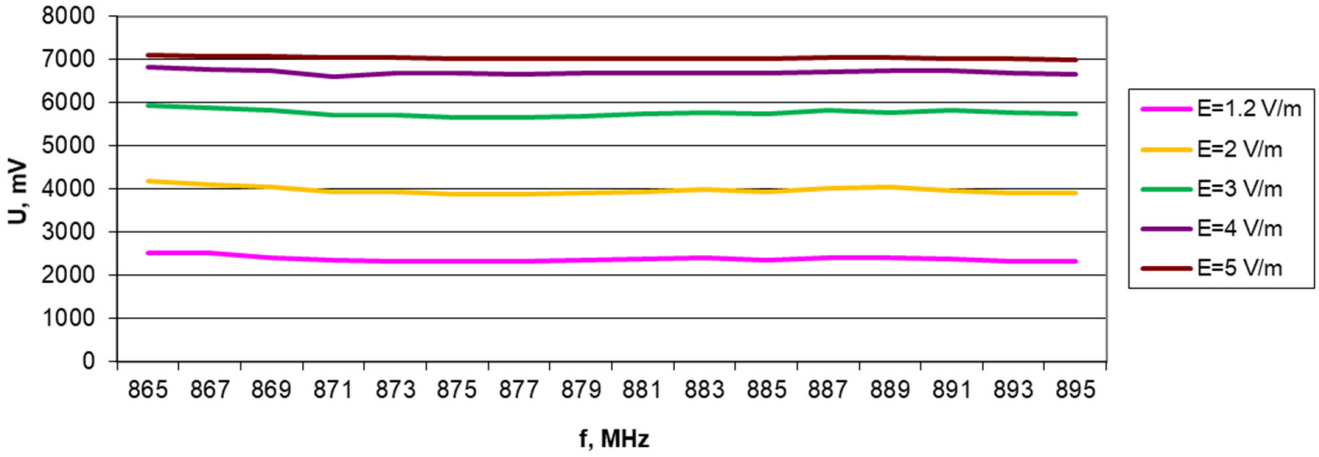

Figure 19. Results of unloaded harvester output voltage measurements for the Europe RFID/GSM 850 band (downlink) as a function of changes in field strength for antenna A6.

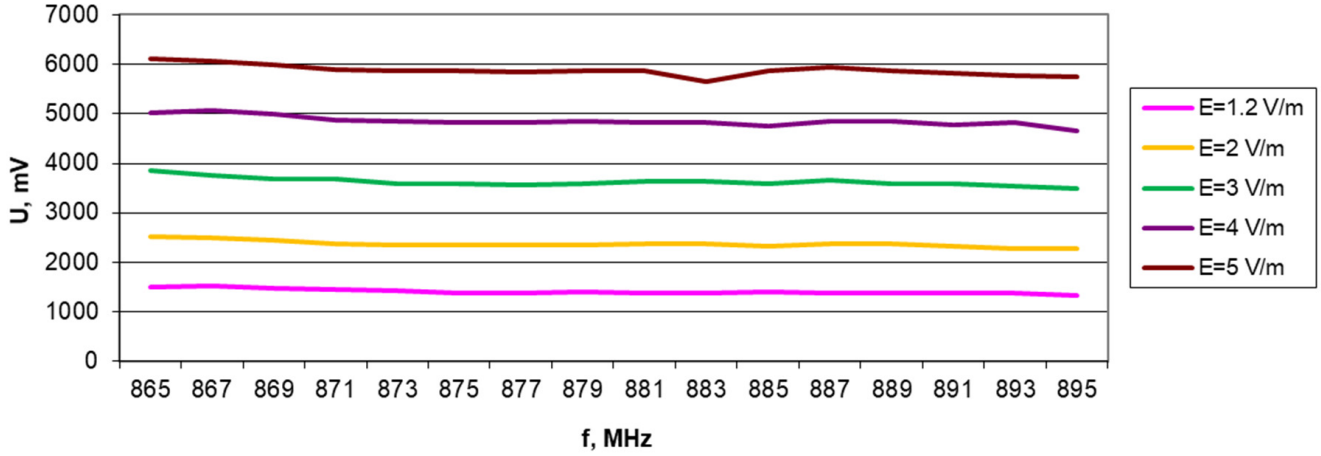

Figure 20. Results of harvester output voltage measurements with 15 kΩ load for the Europe RFID/GSM 850 band (downlink) as a function of changes in field strength for antenna A6.

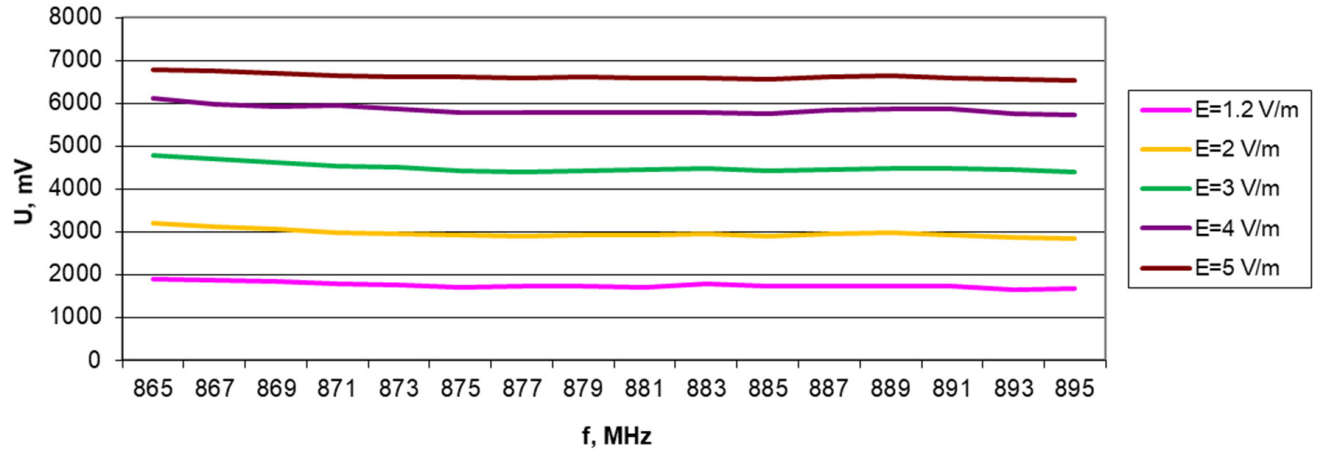

Figure 21. Results of harvester output voltage measurements with 30 kΩ load for Europe RFID/GSM 850 band (downlink) as a function of changes in field strength for antenna A6.

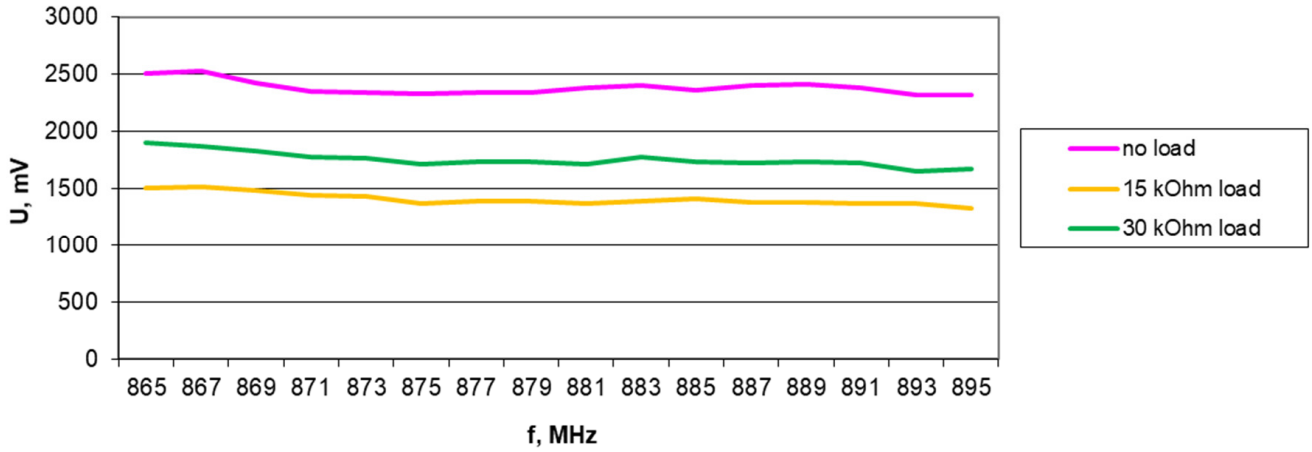

Figure 22. Results of harvester output voltage measurements without load, with 15 kΩ, and with 30 kΩ load for the Europe RFID/GSM850 band (downlink) in 1.2 V/m electromagnetic field for A6 antenna.

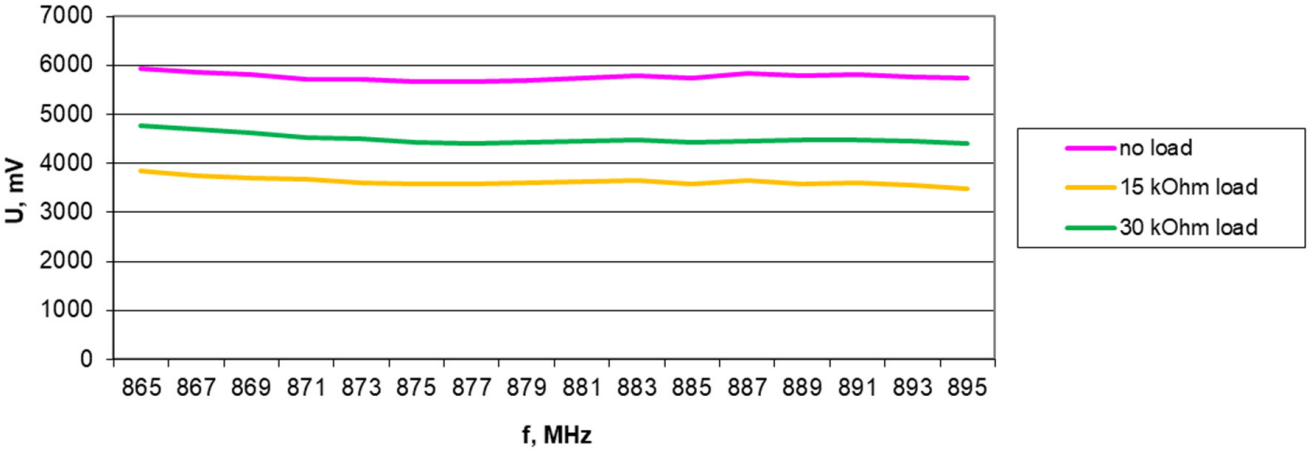

Figure 23. Results of harvester output voltage measurements without load, with 15 kΩ, and with 30 kΩ load for Europe RFID/GSM850 band (downlink) in 3 V/m electromagnetic field for A6 antenna.

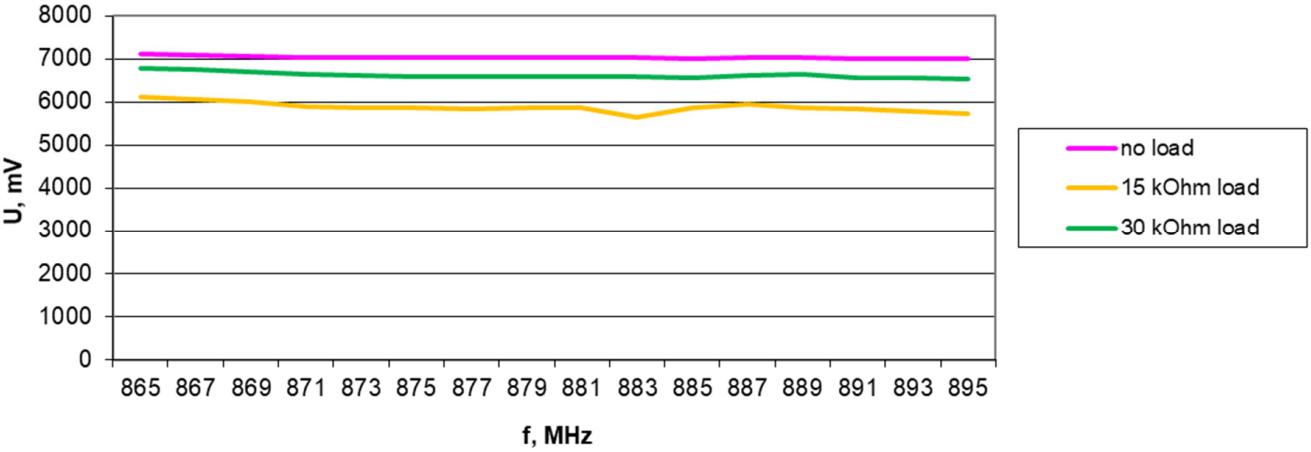

Figure 24. Results of harvester output voltage measurements without load, with 15 kΩ, and with 30 kΩ load for the Europe RFID/GSM850 band (downlink) in a 5 V/m electromagnetic field for the A6 antenna.

Analyzing the test results, several conclusions can be drawn. Given the specifics of the operation of the harvester system in the target application system, which will hardly

require a properly orientated directional antenna to the potential source of the recovered energy, a critical aspect in the design of the identifier system is the proper selection of the antenna of the receiver system. This requires reconciling conflicting requirements: ensuring that the antenna has the highest possible energy gain while maintaining its omnidirectional characteristics. The second alternative is to configure each system of this type to operate under specific field conditions. The results clearly underscore the importance of maintaining optimal parameters for the energy recovery channel to achieve optimal output voltage, which is similar to requirements in typical telecommunications channels.

5. Analysis of the Operation of the Harvester System as a Power Source

To conduct a more detailed analysis of the operation of the harvester system, numerous factors would have to be considered, and this significantly complicates the issue. In the simplest scenario, the system of the tested harvester can be modeled as a voltage source E with series resistance R_{ZR} (Figure 25). The value of the voltage source E in this system depends heavily on the environmental conditions, i.e., the strength and frequency of the electromagnetic field. By recording results of voltage measurements of the tested harvester operating under the same conditions with and without a load, the values of the internal resistance of the source for the applied model of the harvester system can be determined. It is also possible to determine the power dissipated at the attached loads and the impedance matching of the power and load systems. It is important to note that the R_{ZR} of the harvester is a highly nonlinear parameter, influenced by the system design, the energy supply, the antenna used, and the load stage.

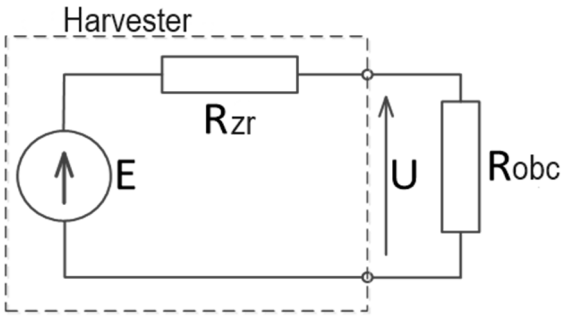

Figure 25. Simplified model of the harvester system.

The selected characteristics of the variation in the resistance of the adopted surrogate source and the power dissipated at the load of the tested harvester, considering changes in the system operating frequency and the available electromagnetic field strength in the surrounding environment, have been shown in Figures 26–40.

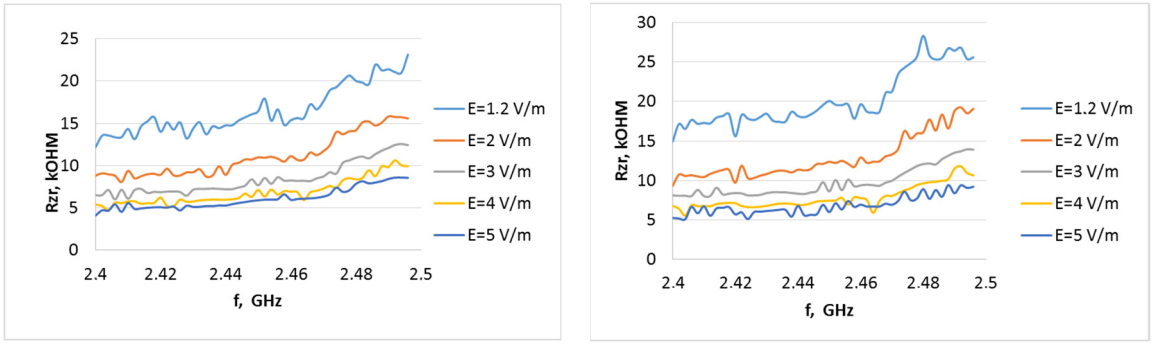

Figure 26. Internal resistance of the P21XXCSR harvester system as a function of frequency from 2.4 to 2.495 GHz (WiFi) at different field strength levels for the A3 type antenna when the system output is loaded with resistance: (**a**) 15 kΩ, (**b**) 30 kΩ.

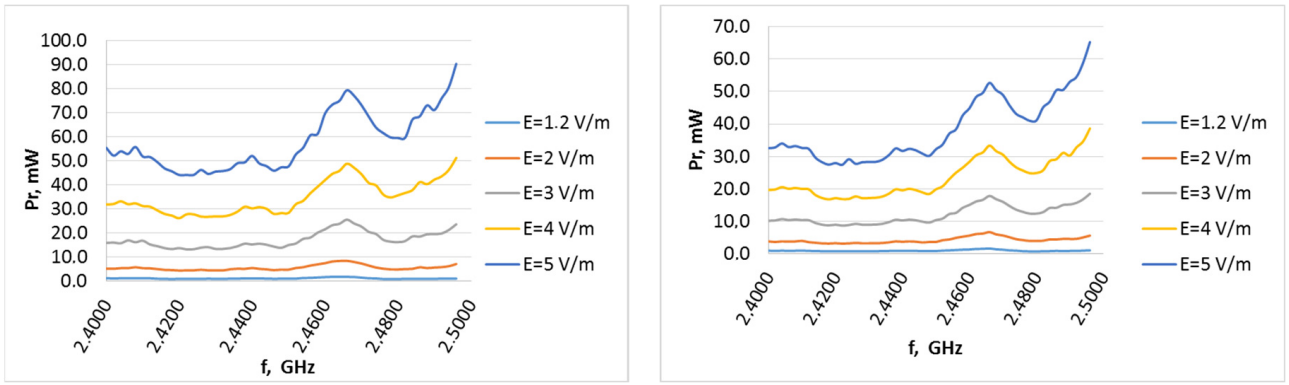

Figure 27. Harvester output power on load (**a**) 15 kΩ and (**b**) 30 kΩ as a function of frequency from 2.4 to 2.495 GHz (WiFi) at different electric field strengths for antenna type A3.

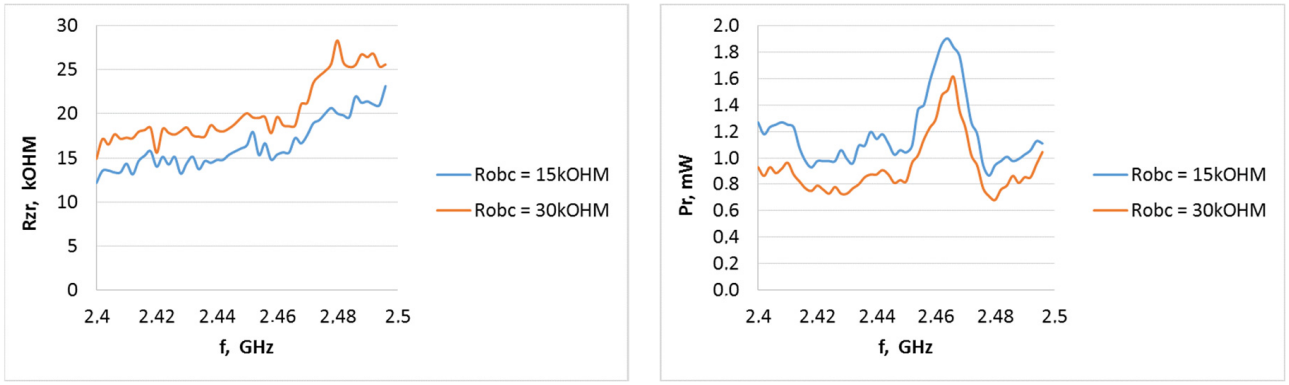

Figure 28. Internal resistance of the P21XXCSR circuit (**a**) and harvester output power at variable loads (**b**) as a function of frequency from 2.4 to 2.495 GHz (WiFi) when operating in an electric field of 1.2 V/m using an A3 type antenna.

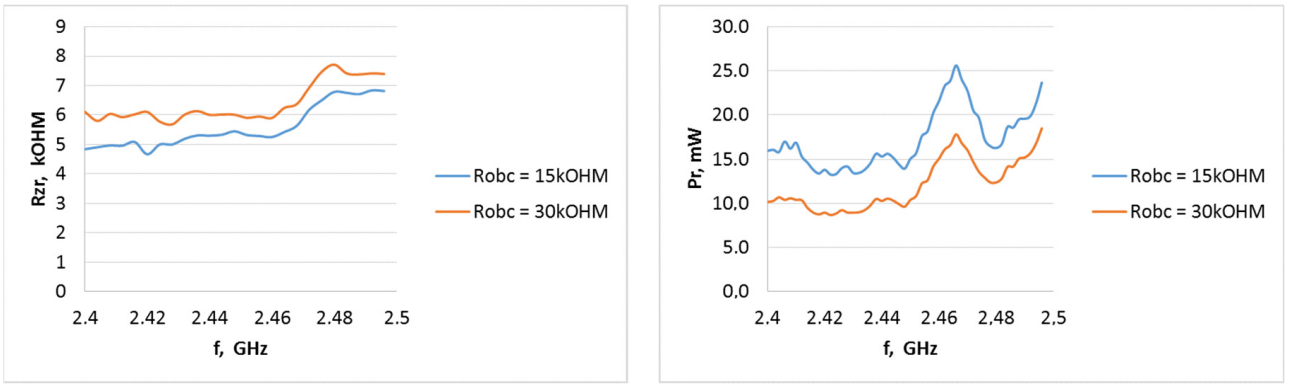

Figure 29. Internal resistance of the P21XXCSR circuit (**a**) and harvester output power at variable load (**b**) as a function of frequency from 2.4 to 2.495 GHz (WiFi) when operating in a 3 V/m electric field using an A3 antenna.

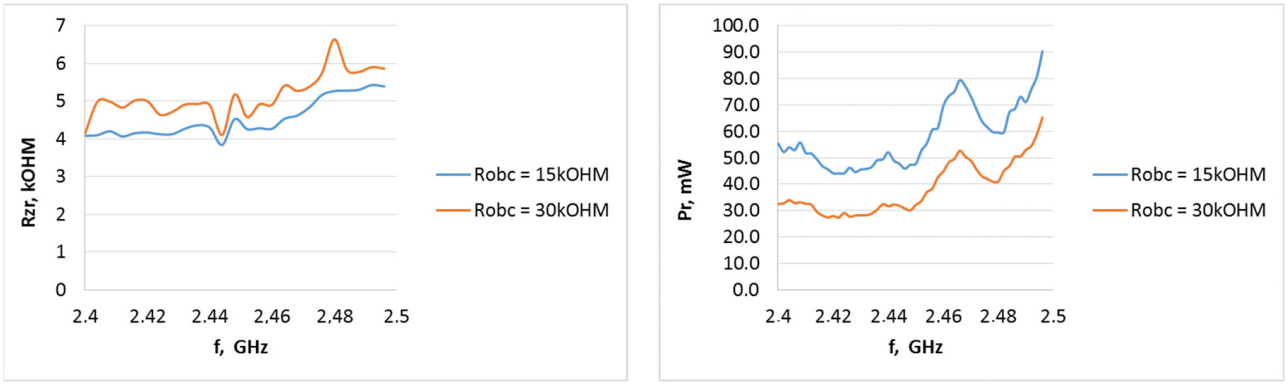

(**a**) (**b**)

Figure 30. Internal resistance of the P21XXCSR circuit (**a**) and harvester output power at variable load (**b**) as a function of frequency from 2.4 to 2.495 GHz (WiFi) when operating in an electric field of 5 V/m using an A3 type antenna.

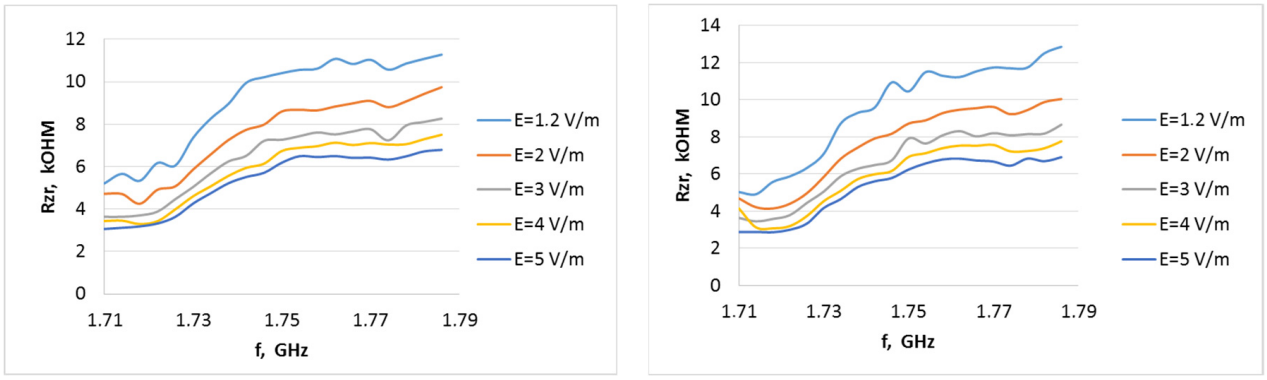

(**a**) (**b**)

Figure 31. Internal resistance of the P21XXCSR harvester system as a function of frequency from 1.710 to 1.785 GHz 1800GSM uplink at different field strength levels for an A5 type antenna when the system output is loaded with resistance: (**a**) 15 kΩ, (**b**) 30 kΩ.

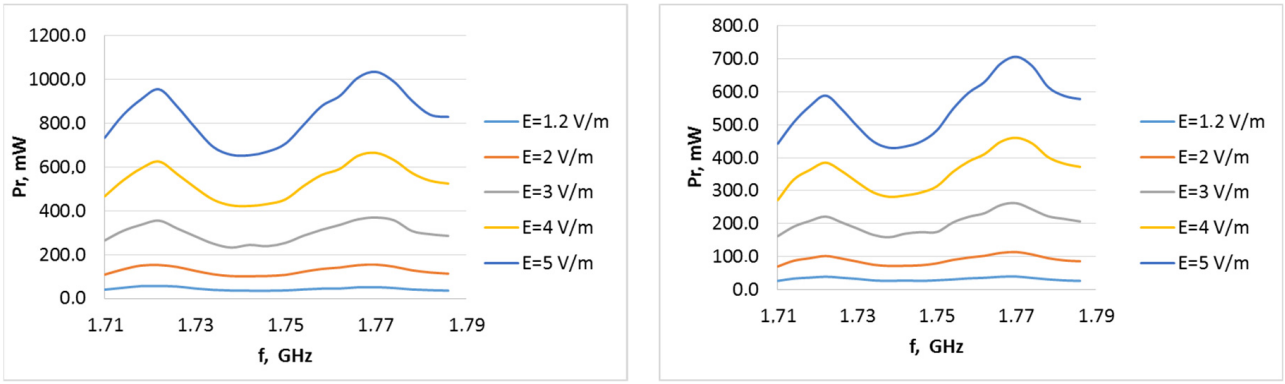

(**a**) (**b**)

Figure 32. Harvester output power on load (**a**) 15 kΩ and (**b**) 30 kΩ as a function of frequency from 1.710 to 1.785 GHz 1800GSM uplink at different electric field strengths for antenna type A5.

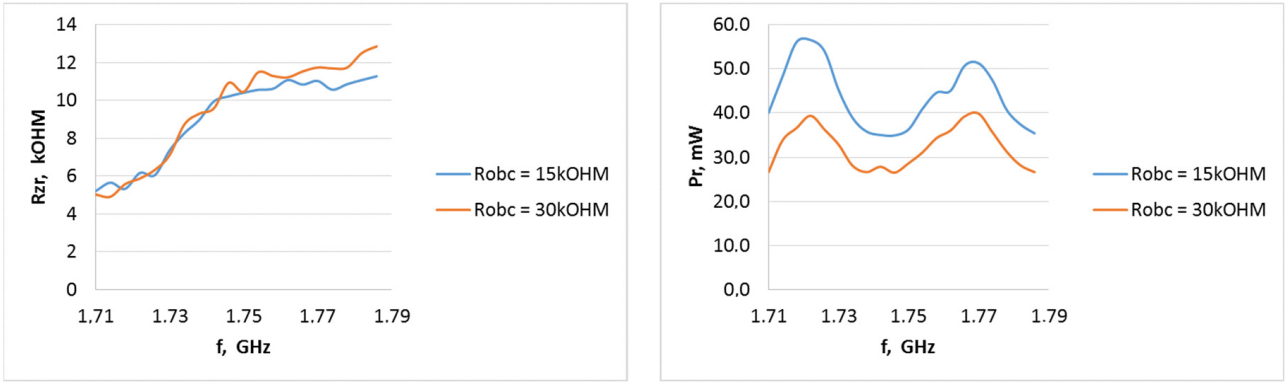

(**a**) (**b**)

Figure 33. Internal resistance of the P21XXCSR circuit (**a**) and harvester output power at variable load (**b**) as a function of frequency from 1.710 to 1.785 GHz 1800GSM uplink when operating in an electric field of 1.2 V/m using an A5 type antenna.

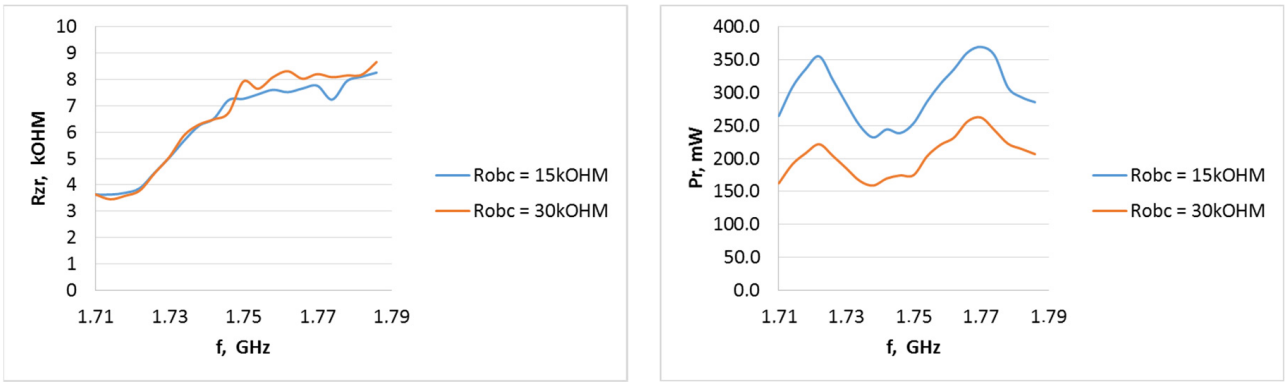

(**a**) (**b**)

Figure 34. Internal resistance of the P21XXCSR circuit (**a**) and harvester output power at variable load (**b**) as a function of frequency from 1.710 to 1.785 GHz 1800GSM uplink when operating in an electric field of 3 V/m using an A5 type antenna.

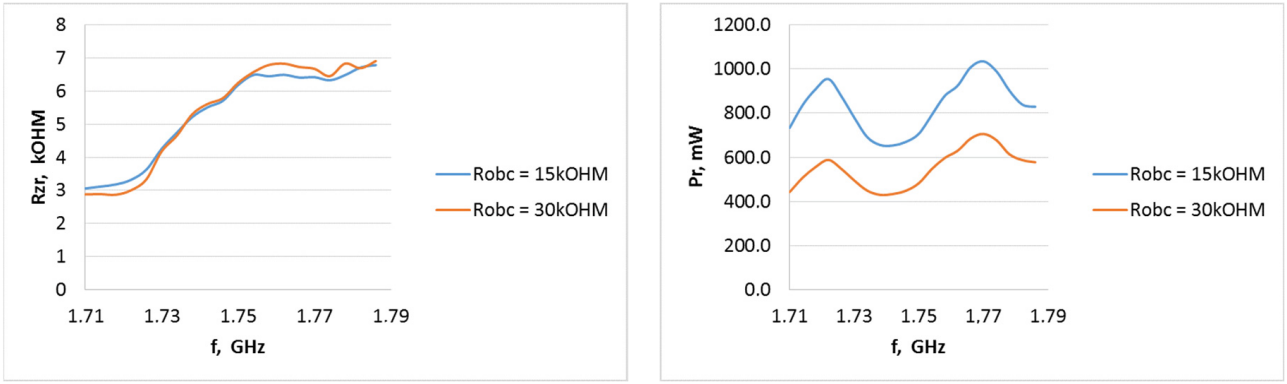

(**a**) (**b**)

Figure 35. Internal resistance of the P21XXCSR circuit (**a**) and harvester output power at variable load (**b**) as a function of frequency from 1.710 to 1.785 GHz 1800GSM uplink when operating in an electric field of 5 V/m using an A5 type antenna.

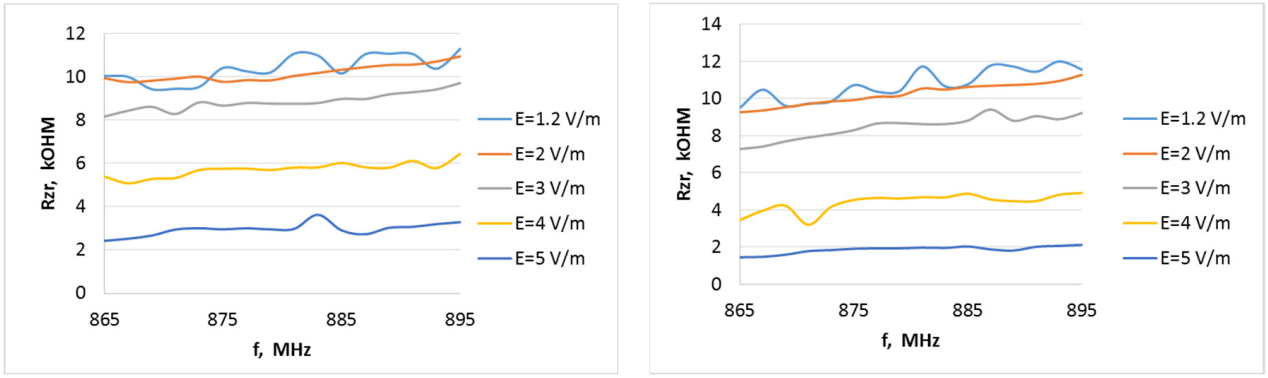

Figure 36. Internal resistance of the P21XXCSR harvester system as a function of frequency from 865 to 895 MHz (Europe RFID/GSM 850 downlink) at different field strength levels for the A6 type antenna when the system output is loaded with resistance: (**a**) 15 kΩ, (**b**) 30 kΩ.

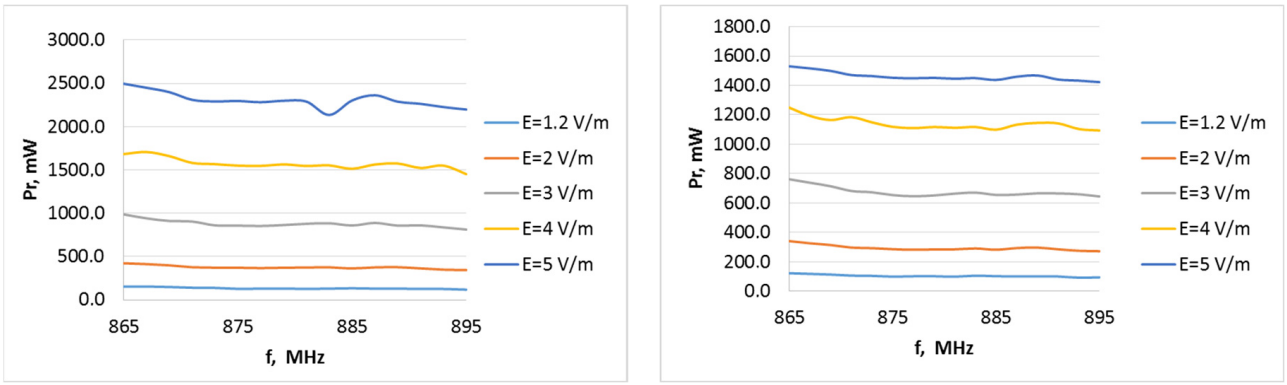

Figure 37. Harvester output power on load (**a**) 15 kΩ and (**b**) 30 kΩ as a function of frequency from 865 to 895 MHz (Europe RFID/GSM 850 downlink) at different electric field strengths for antenna type A6.

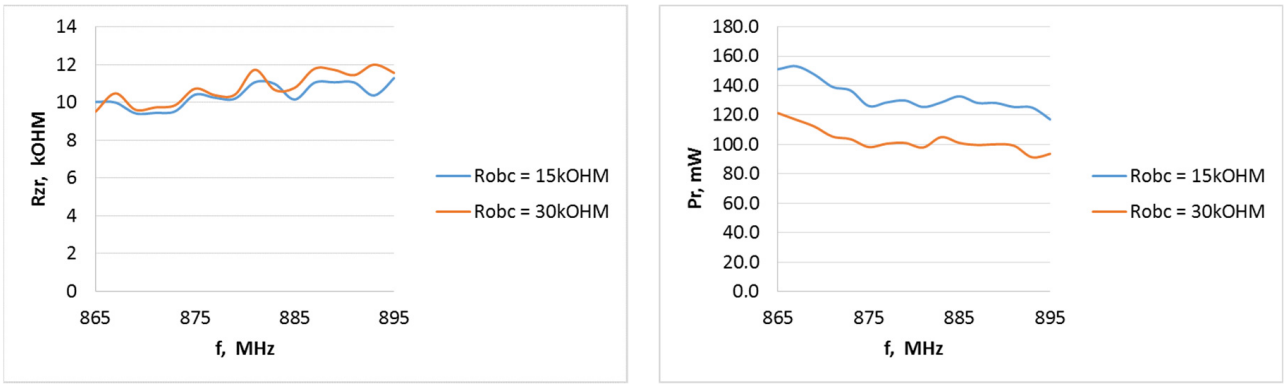

Figure 38. Internal resistance of the P21XXCSR chip (**a**) and harvester output power at variable load (**b**) as a function of frequency from 865 to 895 MHz (Europe RFID/GSM850 downlink) when operating in an electric field of 1.2 V/m using an A6 type antenna.

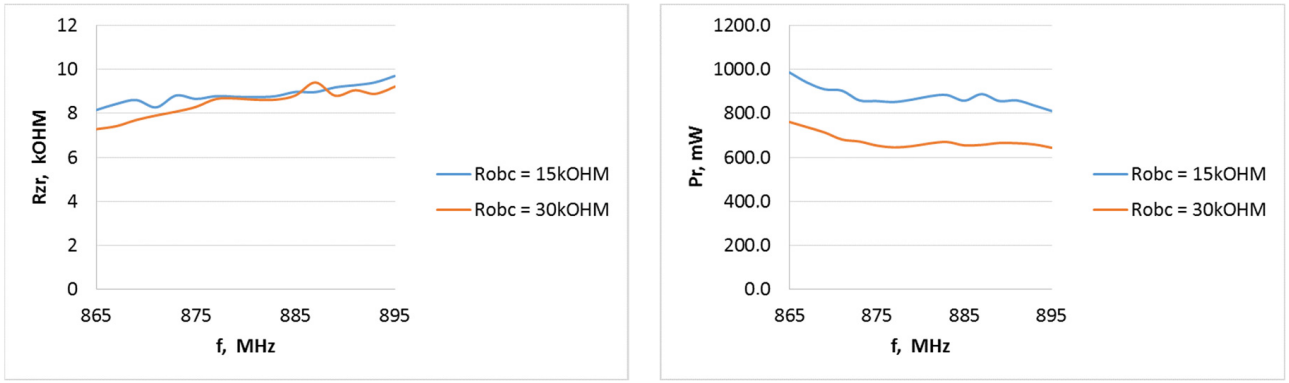

(**a**) (**b**)

Figure 39. Internal resistance of the P21XXCSR circuit (**a**) and harvester output power at variable load (**b**) as a function of frequency from 2.4 to 2.495 GHz (WiFi) when operating in an electric field of 3 V/m using an A6 type antenna.

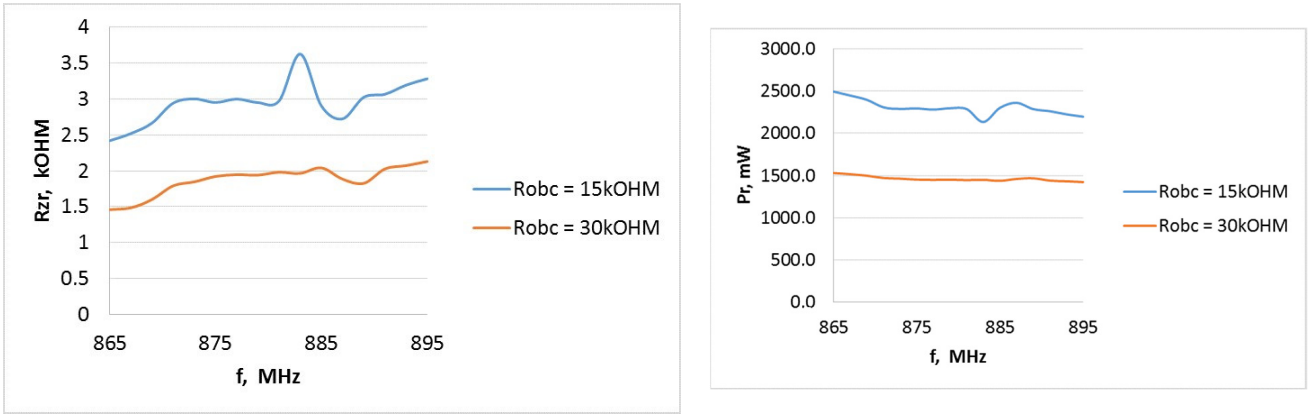

(**a**) (**b**)

Figure 40. Internal resistance of the P21XXCSR chip (**a**) and harvester output power at variable load (**b**) as a function of frequency from 865 to 895 MHz (Europe RFID/GSM850 downlink) when operating in an electric field of 5 V/m using an A6 type antenna.

A harvester is a system designed to supply energy extracted from the environment. Based on the conducted analyses, it is evident that the determined values of the internal resistance of such source vary significantly. This variability is influenced by several factors, primarily the frequency and intensity of the ambient electromagnetic field. Higher values of the electromagnetic field strength of the identifier's operating environment lead to the higher amount of energy recovered and the lower values of the internal resistance of the tested harvester. Conversely, lower field strength values lead to higher values of the determined internal resistance of the source. Therefore, it is crucial under such conditions to properly match the impedance of the identifier circuits to the output resistance of the harvester to achieve maximum possible efficiency of the harvesting process. Additionally, selecting the appropriate harvester antenna for specific operating conditions is equally important.

The issue of impedance matching can be analyzed using the frequency and electric field strength dependence curves of the power dissipated at the load. One can observe that only at certain frequencies can the maximum power output of the source be achieved. The calculated internal resistances of the model source for the same field frequencies reach minimum values. This proves the importance of properly tuning the energy harvesting system to a specific frequency.

The above analyses provide a detailed understanding of the behavior of the energy recovery system, particularly in the estimating of the achievable power output, which is crucial in the design process of a model identifier system. However, they do not account for the behavior of the receiver system under dynamic conditions, given the concept of the system requires conditioning for the parameters of the recovered energy and its storage. This mode of operation will serve as the primary one for the harvester system due to the dynamic variation in input parameters within the energy conditioning system's converter, which is primarily dependent on the converter's input voltage and load current. Additionally, the energy storage system, whether centralized or distributed, typically includes capacitive elements such as capacitors and supercapacitors. Hence, the dynamic parameters of the energy recovery system were also explored at this stage, including the assessment of dynamic charging characteristics across different capacitor types and capacitance values. This investigation aimed to ascertain the actual energy harvesting and storage capabilities of the target system (including energy quantity and storage duration) and to optimize the structure of the energy conditioning and retention system. Capacitors of varying capacitances were sequentially connected to the harvester system's output, and the charging process was conducted under varying field strengths. Measurements were conducted for capacitors with capacitances of 10 µF, 100 µF, and 1000 µF for the harvester configuration cooperating with the A5 antenna for all tested bands (the broadband A5 antenna was treated as a reference antenna).

Examples of the dynamic results of the processes that occur when energy is stored in a capacitor on the ete that mediates its transfer from the harvester to the inverter are shown in Figures 41–49. The capacitance of this capacitor, as well as the voltage levels to which it will be charged and discharged by the inverter, play a major part in the entire system's operation. Therefore, it is crucial to determine the principles of selecting such capacitor and its voltage charge range, to ensure maximum efficiency of the entire energy harvesting system. Powercast Corp.'s P21XXCSR harvester module, as designed, can charge the buffer capacitor in one of three voltage ranges: 0.64–0.738 V, 0.9–0.945 V, and 1.02–1.25 V [18]. Tables 3–5 present the dynamic resistance values determined for these conditions based on the waveforms of charging characteristics of various capacitors in the given ranges of operating voltages (only for those parts of the characteristics where it was feasible to determine the value of this parameter).

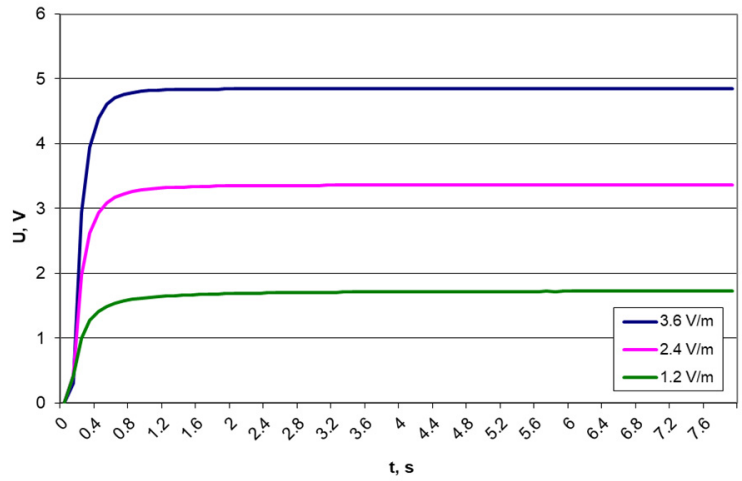

Figure 41. Results of voltage measurements on a 10 µF capacitor for different electric field strengths and a frequency of 879.5 MHz.

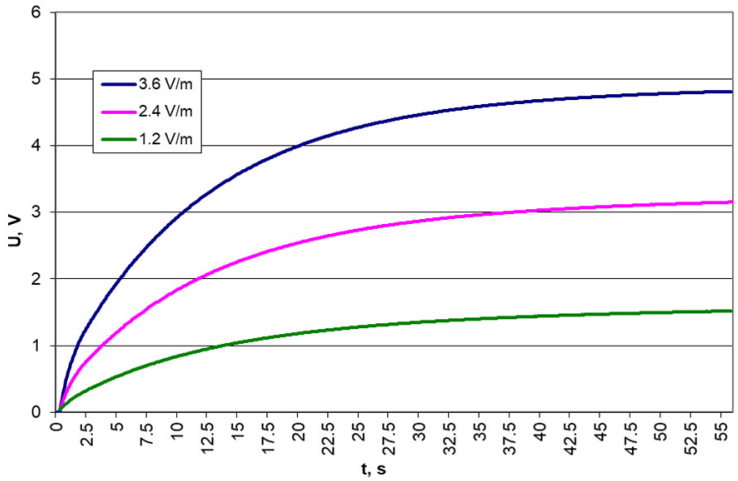

Figure 42. Results of voltage measurements on a 100 μF capacitor for different electric field strengths and a frequency of 879.5 MHz.

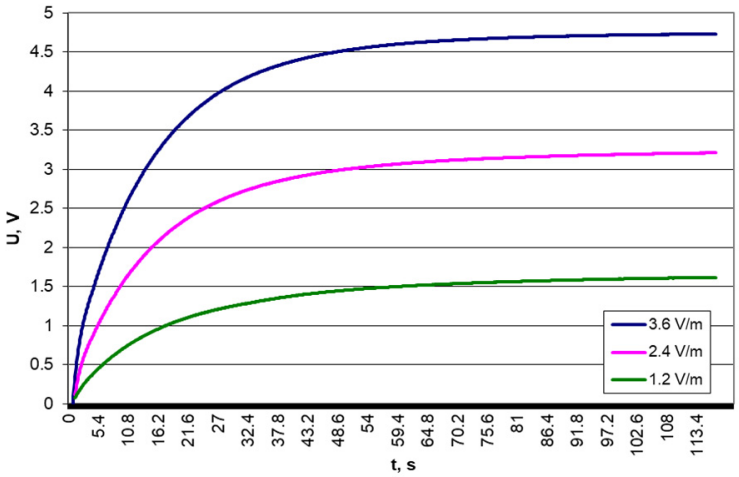

Figure 43. Results of voltage measurements on a 1000 μF capacitor for different electric field strengths and a frequency of 879.5 MHz.

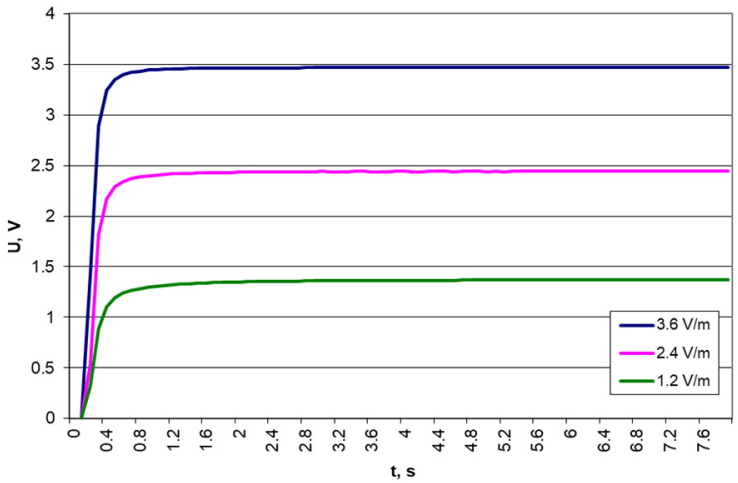

Figure 44. Results of voltage measurements on a 10 μF capacitor for different electric field strengths and a frequency of 1747.5 MHz.

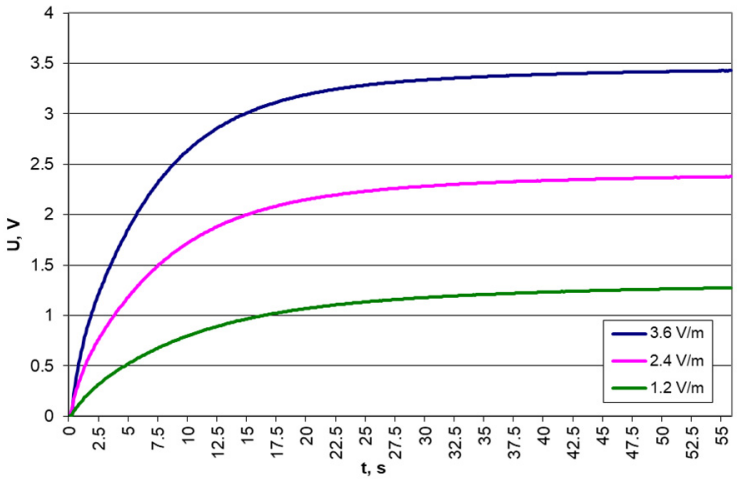

Figure 45. Results of voltage measurements on a 100 μF capacitor for different electric field strengths and a frequency of 1747.5 MHz.

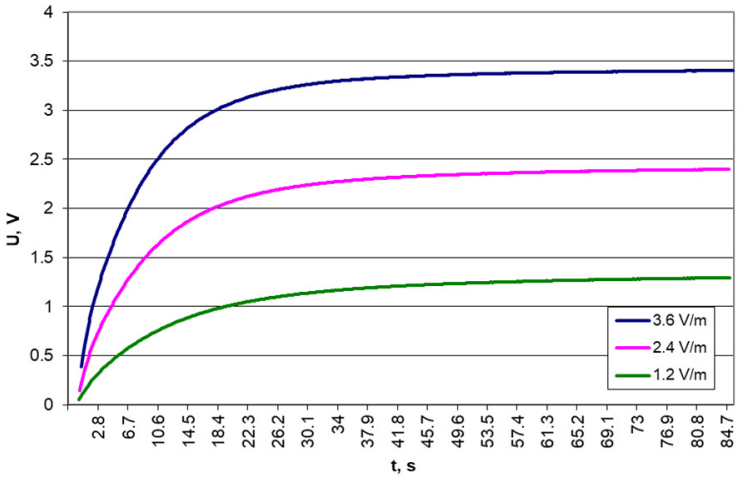

Figure 46. Results of voltage measurements on a 1000 μF capacitor for different electric field strengths and a frequency of 1747.5 MHz.

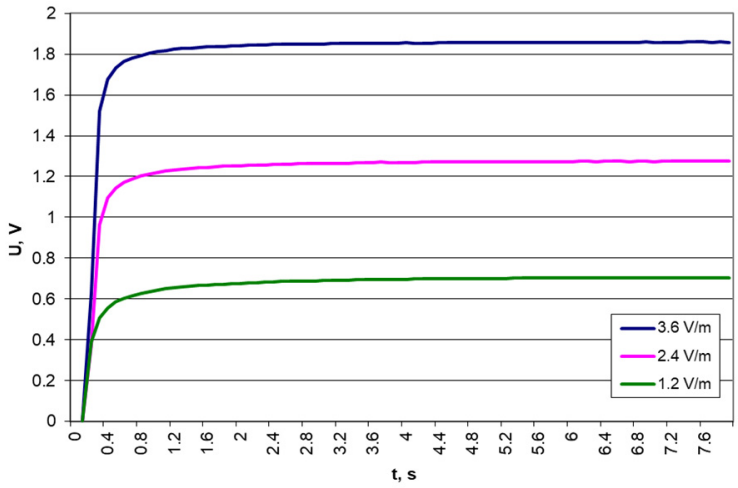

Figure 47. Results of voltage measurements on a 10 μF capacitor for different electric field strengths and a 2442 MHz frequency.

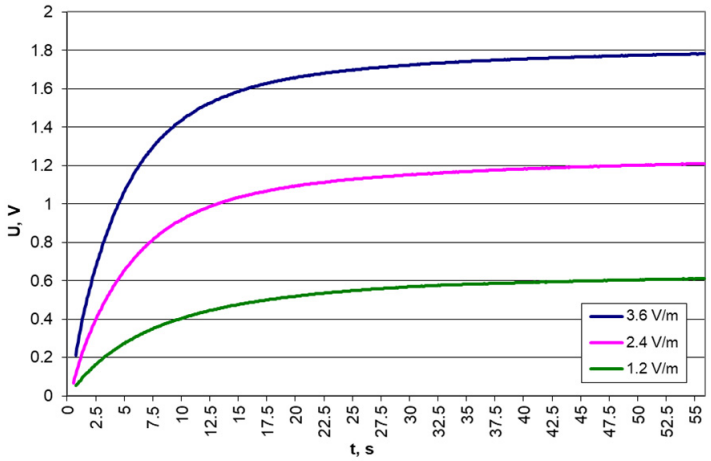

Figure 48. Results of voltage measurements on a 100 µF capacitor for different electric field strengths and a 2442 MHz frequency.

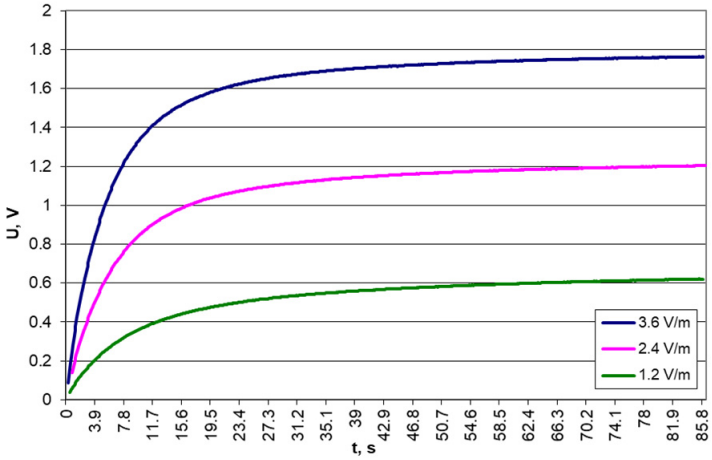

Figure 49. Results of voltage measurements on a 1000 µF capacitor for different electric field strengths and a 2442 MHz frequency.

Table 3. Dynamic resistance R_D of the P21XXCSR harvester system operating in the voltage range 0.9–0.945 V when charging a capacitor of fixed capacitance for different field strength levels.

		1.2 V/m	2.4 V/m	3.6 V/m
C, µF	**f, MHz**	**R_D, kΩ**	**R_D, kΩ**	**R_D, kΩ**
10	836.5	1.29	0.86	0.22
	879.5	1.72	0.86	0.22
	947.5	0.65	0.65	0.65
	1747.5	1.72	0.86	0.86
	1815	1.72	0.86	0.43
	2442	173.05	1.81	1.03
100	836.5	-	-	-
	879.5	14.77	4.67	1.66
	947.5	8.59	2.56	1.05
	1747.5	17.63	4.37	1.96
	1815	22.75	4.52	2.11
	2442	-	12.91	4.82

Table 3. *Cont.*

		1.2 V/m	2.4 V/m	3.6 V/m
C, μF	**f, MHz**	**R_D, kΩ**	**R_D, kΩ**	**R_D, kΩ**
1000	836.5	-	0.92	-
	879.5	1.95	0.52	0.19
	947.5	1.03	0.32	0.13
	1747.5	2.07	0.48	0.19
	1815	2.78	0.54	-
	2442	-	1.59	0.59

Table 4. Dynamic resistance R_D of the P21XXCSR harvester system operating in the voltage range of 1.02–1.25 V when charging a capacitor of fixed capacitance for different field strength levels.

		1.2 V/m	2.4 V/m	3.6 V/m
C, μF	**f, MHz**	**R_D, kΩ**	**R_D, kΩ**	**R_D, kΩ**
10	836.5	-	-	0.08
	879.5	0.86	0.22	0.22
	947.5	0.43	0.43	0.43
	1747.5	2.15	0.43	0.21
	1815	2.80	0.22	0.22
	2442	-	-	-
100	836.5	5.12	-	0.08
	879.5	10.25	2.41	1.05
	947.5	4.97	1.51	0.75
	1747.5	14.46	2.26	1.36
	1815	-	2.56	1.21
	2442	-	14.12	2.76
1000	836.5	0.76	-	0.08
	879.5	1.17	0.26	0.04
	947.5	0.58	0.19	0.06
	1747.5	0.43	0.32	0.13
	1815	4.69	0.28	0.11
	2442	-	1.83	0.35

Based on of the measurement data, it is evident that the most efficient operation occurs when the harvester charges the capacitor in the voltage range of 0.9–0.945 V, as this range corresponds to the lowest dynamic resistance values. The choice of buffering capacitance depends on the electromagnetic field strength around the antenna and the harvester. Analyzing the results further reveals that the lowest values of the dynamic resistance of the harvester system occurred when the tested harvester was loaded with 1000 μF capacitance. Given the observed variability in the parameters of the harvester treated as a power source, it is also worth considering the possibility of designing an inverter with the function of optimizing the impedance matching of such source to the load in the Maximum Power Point Tracking (MPPT) mode (similar to that used in photovoltaic installations). However, definitive conclusions could only be drawn after testing a harvester system integrated with an inverter capable of recharging the main energy storage such as a supercapacitor.

Table 5. Dynamic resistance R_D of the P21XXCSR harvester system operating in the voltage range 1.02–1.25 V when charging a capacitor of constant capacitance for different field strength levels.

		1.2 V/m	2.4 V/m	3.6 V/m
C, μF	**f, MHz**	**R_D, kΩ**	**R_D, kΩ**	**R_D, kΩ**
10	836.5	-	-	-
	879.5	8.39	1.72	0.86
	947.5	1.51	1.51	1.51
	1747.5	11.19	1.72	1.72
	1815	-	1.94	1.51
	2442	-	-	-
100	836.5	31.94	0.00	4.52
	879.5	68.10	13.26	5.88
	947.5	31.49	9.04	4.07
	1747.5	123.70	14.31	6.93
	1815	-	15.82	6.78
	2442	-	156.01	19.11
1000	836.5	3.86	-	0.28
	879.5	3.86	1.69	0.84
	947.5	4.20	1.07	0.52
	1747.5	14.88	1.84	0.87
	1815	-	1.81	0.82
	2442	-	23.38	2.34

6. Conclusions

The concept and the findings of comprehensive investigation of the performance of an energy recovery system (harvester) developed in collaboration with Powercast Corp. are presented in this paper. The harvester system was adapted to European conditions, enabling utilization across a broad spectrum of radio bands commonly used in general-purpose telecommunications systems. Particular emphasis was given to mapping the parameters of the electromagnetic field in laboratory settings, aligning them with typical real-world application scenarios and current regulatory standards. This is crucial for obtaining full information about the energy harvesting capabilities under specific environmental, system, and configuration conditions corresponding to the real world. The investigated harvesters were treated as unconventional power supplies, which, despite unknown and dynamically variable output parameters (voltage, power, internal resistance, etc.), aimed to ensure the operation of the powered system according to the developed concept and scenario of its operation. In this particular case, it was a model semi-passive RFID tag chip, but it could be any other electronic circuit, e.g., an RFID tag, a wireless sensor, a sensor network element, etc. This study includes a brief description of a new prototype harvester system with an output voltage circuit, highlighting selected hardware parameter configurations for testing and verifying its correct operation. This is an alternative, proprietary use of the system for testing the immunity of equipment in the SAC chamber under the EMC directive, with the detailed concept and test results to be addressed in a separate publication.

The concept of a harvester treated as a power supply was substantiated through number of measurements, which serve as the primary sources of data for designing and verifying the target harvester power supply required for selected applications. The voltage performance characteristics of this source were determined for various load resistances. The impact of the capacitance in the indirect energy storage, while directly loading the harvester, on the dynamics and efficiency of energy harvesting was investigated. Furthermore, the

internal resistance of the equivalent source was determined as a function of the frequency and electric field strength feeding the harvester system. The question of matching the load of the harvester under study with its internal resistance in order to maximize the amount of energy harvested was also considered. The detailed results of this study enable us the determine the output voltage dependence of the harvester system under specific application conditions, identification of the minimum power density levels of the target environment to enable the operation of the harvester system, the necessity for proper tuning of the receiver to the frequencies in the band covered by the energy recovery process, and the influence of different types of antennas on the properties and parameters of the system.

Ultimately, these findings facilitate the successful realization of a system for the recovery and storing of energy from the electromagnetic field of general-purpose telecommunications systems. This system aims to power the system of the semi-passive RFID tag under development, or any other system operating under similar conditions based on any other system.

All findings will contribute to a subsequent study focusing on the concept of a harvester with an energy conditioning system, allowing the characteristics of such a system to be universally shaped depending on the requirements and needs of the system being supplied.

Author Contributions: Writing—original draft preparation, conceptualization, methodology: K.K. (Kazimierz Kamuda) and D.K.; writing—and editing: D.K.; resources, validation, formal analysis, investigation, data creation, visualization: W.S., D.K., M.S., K.K. (Kazimierz Kamuda), P.J.-M. and K.K. (Kazimierz Kuryło). All authors have read and agreed to the published version of the manuscript.

Funding: This research paper was developed under the project financed by the Minister of Education and Science of the Republic of Poland within the "Regional Initiative of Excellence" program for years 2019–2023. Project number 027/RID/2018/19. Amount granted PLN 11.999.900. The work was developed by using equipment purchased in the EU programs: POPW.01.03.00-18-012/09-00; UDA-RPPK.01.03.00-18-003/10-00. This work was supported in part by the Polish National Centre for Research and Development (NCBR) under Grant No. PBS1/A3/3/2012.

Data Availability Statement: Data are contained within the article.

Conflicts of Interest: The authors declare no conflicts of interest. The funders had no role in the design of the study; in the collection, analyses, or interpretation of data; in the writing of the manuscript; or in the decision to publish the results.

References

1. Piñuela, M.; Mitcheson, P.D.; Lucyszyn, S. Ambient RF Energy Harvesting in Urban and Semi-Urban Environments. *Trans. Microw. Theory Tech.* **2013**, *61*, 2715–2726. [CrossRef]
2. Visser, H.J.; Vullers, R.J.M. RF Energy Harvesting and Transport for Wireless Sensor Network Applications: Principles and Requirements. *Proc. IEEE* **2013**, *101*, 1410–1423. [CrossRef]
3. Sardini, E.; Serpelloni, M. Passive and Self-Powered Autonomous Sensors for Remote Measurements. *Sensors* **2009**, *9*, 943–960. [CrossRef] [PubMed]
4. Sarker, M.R.; Saad, M.H.M.; Olazagoitia, J.L.; Vinolas, J. Review of Power Converter Impact of Electromagnetic Energy Harvesting Circuits and Devices for Autonomous Sensor Applications. *Electronics* **2021**, *10*, 1108. [CrossRef]
5. Digregorio, G.; Redouté, J.-M. Electromagnetic Energy Harvester Targeting Wearable and Biomedical Applications. *Sensors* **2024**, *24*, 2311. [CrossRef] [PubMed]
6. Kim, S.; Vyas, R.; Bito, J.; Niotaki, K.; Collado, A.; Georgiadis, A.; Tentzeris, M.M. Ambient RF Energy-Harvesting Technologies for Self-Sustainable Standalone Wireless Sensor Platforms. *Proc. IEEE* **2014**, *102*, 1649–1666. [CrossRef]
7. Radhika, N.; Preetika, T.; Prabhakar, T.V.; Vinoy, K.J. RF Energy Harvesting For Self Powered Sensor Platform. In Proceedings of the 16th IEEE International New Circuits and Systems Conference (NEWCAS), Montreal, QC, Canada, 24–27 June 2018; pp. 148–151. [CrossRef]
8. Mouapi, A. Radiofrequency Energy Harvesting Systems for Internet of Things Applications: A Comprehensive Overview of Design Issues. *Sensors* **2022**, *22*, 8088. [CrossRef] [PubMed]
9. Lee Yi Ch Ramiah, H.; Choo, A.; Churchill, K.; Kumar, P.; Lai NS Lim Ch Ch Chen, Y.; Mak, P.-I.; Martins, R.P. High-Performance Multiband Ambient RF Energy Harvesting Front-End System for Sustainable IoT Applications—A Review. *IEEE Access* **2023**, *11*, 11143–11164. [CrossRef]
10. Mizeraczyk, J.; Budnarowska, M. Microwave Metamaterial Absorber with Radio Frequency/Direct Current Converter for Electromagnetic Harvesting System. *Electronics* **2024**, *13*, 833. [CrossRef]

11. Mikeka, C.h.; Arai, H. Design Issues in Radio Frequency Energy Harvesting System. In *Sustainable Energy Harvesting Technologies—Past, Present and Future*; Tan, Y.K., Ed.; InTech: Rjeka, Croatia, 2011; pp. 237–256.
12. Batool, U.; Rehman, A.; Khalil, N.; Islam, M.; Afzal, M.U.; Tauqeer, T. Energy extraction from RF/Microwave signal. In Proceedings of the 15th International Multitopic Conference (INMIC), Islamabad, Pakistan, 13–15 December 2012; pp. 165–170. [CrossRef]
13. Hagerty, J.A.; Helmbrecht, F.B.; McCalpin, W.H.; Zane, R.; Popovic, Z.B. Recycling ambient microwave energy with broad-band rectenna arrays. *IEEE Trans. Microw. Theory Tech.* **2004**, *52*, 1014–1024. [CrossRef]
14. Arrawatia, M.; Baghini, M.S.; Kumar, G. RF energy harvesting system from cell towers in 900 MHz band. In Proceedings of the National Conference on Communications (NCC), Bangalore, India, 28–30 January 2011; pp. 1–5. [CrossRef]
15. Taris, T.; Vigneras, V.; Fadel, L. A 900 MHz RF energy harvesting module. In Proceedings of the 10th IEEE International NEWCAS Conference, Montreal, QC, Canada, 17–20 June 2012; pp. 445–448. [CrossRef]
16. Malaeb, M.; Tlili, B. RF Energy Harvesting System for GSM900 and GSM1800 Bands. In Proceedings of the International Conference on Renewable Energy: Generation and Applications (ICREGA), Al Ain, United Arab Emirates, 2–4 February 2021; pp. 9–14. [CrossRef]
17. Keyrouz, S.; Visser, H.J.; Tijhuis, A.G. Ambient RF energy harvesting from DTV stations. In Proceedings of the Loughborough Antennas & Propagation Conference (LAPC), Loughborough, UK, 12–13 November 2012; pp. 1–4. [CrossRef]
18. *802.11-2016*; IEEE Standard for Information Technology—Telecommunications and Information Exchange between Systems Local and Metropolitan Area Networks—Specific Requirements-Part 11: Wireless LAN Medium Access Control (MAC) and Physical Layer (PHY) Specifications. (2016 Revision). IEEE: New York, NY, USA, 14 December. [CrossRef]
19. Olgun, U.; Chen, C.-C.; Volakis, J.L. Efficient ambient WiFi energy harvesting technology and its applications. In Proceedings of the IEEE International Symposium on Antennas and Propagation, Chicago, IL, USA, 8–14 July 2012; pp. 1–2. [CrossRef]
20. Szut, J.; Piątek, P.; Pauluk, M. RF Energy Harvesting. *Energies* **2024**, *17*, 1204. [CrossRef]
21. Sabat, W.; Klepacki, D.; Kamuda, K.; Kuryło, K.; Jankowski-Mihułowicz, P. Efficiency Measurements of Energy Harvesting from Electromagnetic Environment for Selected Harvester Systems. *Electronics* **2023**, *12*, 4247. [CrossRef]
22. Product Datasheet of Evaluation Board for P2110. Available online: https://www.powercastco.com/wp-content/uploads/2021/06/P21XXCSR-EVB-Datasheet-v2.1-1.pdf (accessed on 15 March 2024).
23. Sabat, W.; Klepacki, D.; Kamuda, K.; Kuryło, K. Analysis of Electromagnetic Field Distribution Generated in an Semi-Anechoic Chamber in Aspect of RF Harvesters Testing. *IEEE Access* **2021**, *9*, 92043–92052. [CrossRef]